2016

# COMPARISON OF DIFFERENT SEISMIC FILTERING TECHNIQUES ON PRESTACK INVERSION FOR PENOBSCOT AREA-NOVA SCOTIA

Omer Emre Uygun
*Michigan Technological University*, oeuygun@mtu.edu

# COMPARISON OF DIFFERENT SEISMIC FILTERING TECHNIQUES ON PRESTACK INVERSION FOR PENOBSCOT AREA-NOVA SCOTIA

By

Omer Emre Uygun

A THESIS

Submitted in partial fulfillment of the requirements for the degree of

MASTER OF SCIENCE

In Geophysics

MICHIGAN TECHNOLOGICAL UNIVERSITY

2016

This thesis has been approved in partial fulfillment of the requirements for the Degree of MASTER OF SCIENCE in Geophysics.

Department of Geological and Mining Engineering and Sciences

Thesis Co-Advisor: *Dr. Wayne D. Pennington*

Thesis Co-Advisor: *Dr. Gregory P. Waite*

Committee Member: *Prof. Mir Sadri*

Department Chair: *Dr. John S. Gierke*

Table of Contents

# Acknowledgments

I would like to express my deepest gratitude to my advisor, Dr. Wayne D. Pennington for his support, patience, guidance, and encouragement throughout my study. He has been a great mentor to me. He has spent countless hours for me to have a better thesis. He did not hesitate to spend his time to give me advice on my work. I would like to express my appreciation to my co-advisor Dr. Gregory P. Waite for his support and suggestions. I also would like to thank Prof Mir Sadri for being on my committee.

The dataset is used used in this thesis is provided by dGB Earth Sciences, makers of OpendTect, and the processing is performed with Geoview software form Hampson-Russel. I appreciate their support.

I would like to thank Turkish Petroleum Corporations (TPAO) for their financial support. It is an honor to have this scholarship.

My appreciation also goes to my friend Ceyda Karatas. She has helped me and supported me throughout my thesis. Also, I appreciate my numerous friends who have supported me throughout this process.

Above all, my biggest gratitude goes to my family. I cannot express how grateful I am to have them, my sister Ayse Gulce Uygun, my mother Zehra Uygun, and my father Ismail Bulent Uygun. I have felt their support, encouragement, suggestions, and love every day and at every time in my life. I would not be me if it was not for them.

Finally, I would like to thank my grandparents, Zehra Uygun, Huseyin Uygun, Sehriban Asikoglu, and Recep Nihat Asikoglu. They have taught me, and supported me in my life. Rest in peace.

# Abstract

The goal of this study is to compare three different type of seismic filtering according to their inversion results and their quality of data improvements. To do this bandpass filter, Inverse Q, and Radon transform are applied to the original NMO corrected pre-stack data from Nova-Scotia offshore Canada.

The seismic data used was provided as pre-stack data of generally good quality. The test for quality of data improvement comes from the results of inversion based on different types of filtering performed on the pre-stack gathers.

Bandpass filter, Inverse Q, and Radon transform are applied to the migrated prestack data, over the time range of 0-6000 ms. The Radon transform yields a better seismic image than the bandpass and inverse Q filters, since it removes the noise and the multiples from the data quite efficiently. The respective data volumes were inverted for acoustic impedance using simultaneous prestack inversion. The Radon filtered data provided the best inversion results, based on the continuity of layers and lack of apparent artifacts or noise. The Radon filter does not appreciably alter the frequency content of the data while removing events with moveout inconsistent with primary arrivals. It is likely that the processed data provided originally contained an excellent wavelet, and the other filters were unable to improve upon it, but did diminish the information present, particularly at the lower frequencies, decreasing the quality of the inversion results.

# 1. Introduction

The purpose of this thesis is to compare and evaluate different prestack seismic filtering techniques and their responses applied to seismic data of the Penobscot area, offshore Nova Scotia. The quality of the final seismic image is crucial for interpretation. While some filtering is routinely performed on poststack seismic data, this thesis concentrates on three specific techniques for improving prestack data. Here, these signal filtering techniques are applied to pre-stack 3D marine seismic data of the Penobscot 3D Survey, publicly accessible through OpendTect website (with the complete pre-stack, post-stack and well data, owned by Nova Scotia Department of Energy). Data provided had already been moved out according to the velocity analysis performed by a contractor. The 3D seismic survey area covers around 90 $km^2$, and is located in offshore Nova Scotia, Canada, on the Scotian Shelf (Figure 1). Table 1 shows the seismic data parameters for the research area. There are two drilled wells in the Penobscot survey area by Petro-Canada & Shell. Penobscot L-30 was drilled in 1976 to 4237.5m and Penobscot B-41 in 1977 to 3414.4m. Non-commercial hydrocarbons were discovered.

Several factors can affect the data quality during acquisition, including environmental and instrumental effects. In addition, while some contaminating effects can be minimized through the use of wisely chosen source and receiver-group designs, or accurate velocity analyses to reduce the effect of multiples, noise remains in the final stack. To the extent that noise can be differentiated from signal, in some domain, it can be reduced through data processing. In this study, bandpass frequency filtering, inverse Q transform and Radon transform have been applied to prestack Penobscot seismic data to improve inversion results for use in seismic interpretation.

Figures 2 and 3 show the amplitude spectrum and example common-mid-point (CMP) gathers from the original prestack seismic data. The gathers exhibit some coherent noise (multiples) with moveout that is different from that used for normal moveout (NMO) correction, and they show some random noise reducing the coherence of amplitudes across the gathers. In simultaneous (prestack) inversion, the change in amplitudes as a function of offset or angle is used to determine elastic properties of the beds between reflections. For the purposes of this study, we will concentrate on the effectiveness of different prestack filtering techniques in producing improved acoustic impedance volumes for interpretation.

Seismic filtering and inversion are applied to the entire seismic volume between the intervals listed in Table 1. However, for the purposes of clarity in this publication, the figures will show seismic data and inversion results from one inline (1177) passing through well L-30.

The methods investigated here include bandpass filtering, inverse-Q filtering, and Radon filtering. For each of these filtering techniques, tests of the various parameters applicable to each are applied, including some values that are extreme, in order to observe the effects clearly. In the main text, the "optimal" values are carried through, but the other values are demonstrated in the appendix for comparison.

# 2. Seismic Filtering

This chapter gives brief information about different types of filtering techniques. The main purpose of a seismic filter is to remove unwanted effects from the seismic image. These unwanted effects are often called noise, and one source of coherent noise is multiple reflections.

## 2.1. Seismic Noise

Seismic noise is a general description for all the effects on the seismic data that is not wanted. There are different types of noise. While some of them are caused by environmental effects, there are other noise types mostly caused by the geology of the area or the instrument. The quality of the seismic data is crucial for the interpretation step. Improving signal quality while removing these unwanted effects is the main purpose of the seismic processing.

There are typically two general classifications of the noise. One of them is called coherent noise, while the other one is called incoherent or random noise. Coherent noise is generally caused by reflection and refraction, such as surface reflections, and the ground roll, is traceable through different seismic traces. On the other hand, as its name indicates incoherent (or random) noise is untraceable, and is generally due to scattering from distributed heterogeneities or environmental and anthropogenic sources. These noise types may be separated by their frequencies. The coherent noise mostly has low frequencies whereas incoherent noise has high frequencies due to the short path of the radiation in the near surface (Li and Tang, 2005).

In marine seismic data, ultra low frequency acoustic noise, which are between 0.1 and 1 Hz, is often recorded. This low frequency noise is usually associated with seismic wave propagation caused by pseudo-Rayleigh waves. These waves propagate through oceans to land over thousands of kilometers. These waves propagate slower than the shear wave in the crust and usually faster than the speed of sound in water. These

types of seismo-acoustic waves generally cause vertical ground surface displacements and these displacements cause acoustic noise in water which dominate the seismic records (Ardhuin, et al., 2013). It is important to get rid of every kind of frequencies between 0 to 1 Hz in marine data to remove low frequency acoustic noise.

## 2.2. Filtering Techniques

### 2.2.1. Bandpass Filter

To remove the unwanted noise effects from the seismic data for a frequency interval, band pass frequency filtering is used. In order to use a bandpass filter, the frequency range of the data must be decided. So that, unwanted low and high frequency can be removed from the data. Foremost, wanted frequency interval is remained to be processed. For pre-stack inversion low frequency is important, thus low frequencies need to remain. Bandpass filtering the can shift the data in time or phase, but if it is well designed it may not affect the shape of the wavelet (Russell, 1988).

Band pass filters are defined by four variables (Figure 4). “Low cut” is the minimum frequency and below that frequency no signal is retained; low frequencies are gradually admitted up to the value provided for “low pass”. “High cut” is the maximum frequency for a signal and no signal is retained above it; “high pass” is the frequency at which the signal starts to be removed. In the middle, between low pass and high pass is the band of frequencies to be passed at full strength.

In order to choose the preferred bandpass filter for the data, six different frequency intervals were tested as listed in Table 2. Bandpass-5 was chosen as the preferred, because it keeps most of the necessary low and high frequency contents, and removes what appears to be noise. An untested option would have been to apply a high-cut filter only with no removal of low-frequency signals or noise. For the purposes of

this study, the filter chosen was that which mildly reduced the lowest and highest frequencies within the data.

In the Figure 6, original data can be seen on the left side, the plot in the middle shows the preferred bandpass filtered seismic data (Bandpass-5), and the right plot gives the rejected noise after bandpass filtering. Bandpass-5 is chosen as preferred because, it covers the most data as seen in amplitude spectrum (Figure 5), and rejects the least favorable data while removing noise. In the Figure „A" shows the multiples and noise rejected. Comparison of the bandpass filter tests, and the original data image is in appendix A.

### 2.2.2. Inverse Q

The inverse Q filtering technique recovers both amplitude decay with frequency and phase changes caused by attenuation as the signal travels through the earth. The attenuation caused by the propagation can be reversed by applying an exponential factor to each harmonic wave component. With inverse Q transformed, the effect of the medium is removed, and high-frequency components are regained (Tu and Lu, 2009).

„Inverse Q-1" is chosen to be the preferred Inverse Q application in this study. In this technique it is important not to alter the data in order to improve signal quality. Too much modification on the signal can cause deviation on the signal and, inverse Q results may get worse. Comparing the tests Inverse Q-1 adds the least extra information to the data as seen in Figure 7, while it removes some of the noise (Figure 8). In the following Figure, multiples and noise added to the data are shown as „A", while „B" shows an apparent improvement of data at the deeper area of interest. The others have overstatements caused by extra information added by not

fitting Q pickings. The comparison of the Inverse Q tests could be found in appendix B.

### 2.2.3. Radon Transform

The Radon transform is useful to filter data in the Radon domain (tau-p) to suppress the effect of the multiples, and other coherent noise. Primary reflections and the multiples can be separated in the Radon domain. If the data is distorted by multiples this technique is highly preferable to get a better seismic image for AVO analysis, or processing procedures like migration (Feng, 2006).

In this study, the parabolic Radon transform is used, applied to the already-moved-out gathers. In the parabolic Radon transform, it is assumed that all gathers can be considered to have been formed as a linear series of parabolic shapes of arrivals of constant amplitude. The Radon parabola is characterized by its amplitude and curvature. The difference in time between the parabola at zero offset and the far offset is called Delta-t, measured in milliseconds. A parabola bends upwards if its Delta-t is negative, and curves downwards if positive. Multiples have positive moveouts, since the Radon transform is generally applied to the NMO corrected data (Russell, 1988).

Figure 9 shows the amplitude spectra for all Radon transform tests and the original data. There is almost no difference in frequency content as a result of any of the Radon filters, as expected. Figure 10 shows the effect of the preferred Radon-1 filter. This filter removes noise, and suppresses the multiples (A), significantly improving the seismic quality. B here shows the apparently unaltered data for the reflection of most interest. The results of the other Radon transform tests can be found in appendix C.

# 3. Inversion

Having selected the preferred bandpass filter, inverse Q, Radon filters, CMP gathers are then stacked. This provides a seismic volume of stacked seismic data, which is ready for conventional modern interpretation, consisting of well-tie and inversion. Although we have started with pre-stack data, and various elastic-property volumes could be created, this study is concerned only with the quality of the inversion results yielding acoustic impedance. A pre-stack inversion process is often used to assist in the interpretation of fluid content and lithologic properties of potential reservoirs.

## 3.1 Well Tie

The main purpose of the well tie is to relate seismic data to the well logs. The correlation between depth and time is one of the important elements that well tie provides (Simm and Bacon, 2014). In this study check-shots were used to correlate time to depth. Synthetic seismograms were generated from density and sonic logs and convolved wavelet. The 10-Hz, 20-Hz, and 25-Hz Ricker wavelets were created. The 25-Hz Ricker wavelet created in the study shows the best relation (Figure 11). During the well tie some stretching and squeezing were applied, but this was kept to a minimum. The correlation at L-30 well for this study is 0.71 (Figure 12). This percentage is adequate enough to get good inversion results, to support comparison of the filtering techniques.

## 3.2. Simultaneous Inversion

Pre-stack inversion can be performed as "simultaneous inversion". To get the best results the inversion process is performed in the angle-gather domain to calculate P-wave impedance ($Z_P$), S-wave impedance ($Z_S$), and density values. First, angle gathers are generated from the NMO migrated gathers. Then, wavelets are extracted for far and near angles from the seismic data. From the logs, P-impedance and density models are created (no shear-wave log was available). A few horizons are tracked in the seismic data, and the log-based models follow these horizons. Inversion analysis is applied as an iterative process to minimize the differences between seismic and synthetics generated from the model, as the model is adjusted accordingly. In the end, two or three elastic volumes are created (Zp and Zs; or Zp, Zs, and density); here we are using only the acoustic impedance (Zp) volume for our test.

Figure 13 shows the simultaneous inversion result for Zp from the original seismic data. This Figure is used to compare the inversion results between filtered and original inversions. The inversion results of bandpass-filtered, inverse-Q filtered, and Radon-filtered inversions are shown in Figures 14, 15, and 16 respectively.

Seismic filtering was necessary to improve the data, since the original inversion is not clear enough to interpret. There are ambiguities in the unfiltered data, because the original data has noise and the multiples contaminated the stacked volume. Inversion results of the original data is less clear than the filtered inversion results, with many discontinuous events and a lack of continuity.

## 3.3. Discussion

While the original data resulted in poor inversion results, the results of the various processing steps provide different inversion results. In Figures 17, 18, and 19 the differences between the original data and the filtered data are showing sections are compared and differences extracted between the original and processed results.

Figure 17 shows the original data inversion, the bandpass filtered inversion, and the differences between these two. In the differences section, no considerable difference is seen for the approximate area of research, horizon-1. The bandpass filter is only limited to the frequency intervals chosen. The shallow part has better than original, because the continuities can be seen.

Figure 18 shows the inversion result for the Inverse Q filter. This inversion is better than the bandpass filter inversion. However, for some parts it adds extra information to the data while removing the attenuation effects. The added extra information may not be correct, and for thin layers it may cause confusion. Inverse Q inversion shows more stratigraphic formation than the bandpass.

Radon inversion demonstrated the best result, since it presents a better lateral continuity and vertical resolution (Figure 19). Thin layers and stratigraphic features are clearly seen and are fairly continuous. The Radon transform is not a frequency filter, like a bandpass filter. It removes the multiples and noise by linearizing the moveouts. The delta intervals of the Radon filter are important at this point, and these are carefully chosen to get better Radon results.

In Figure 20, the differences between inversions of all filters applied can be observed. This Figure supplies better understanding of the differences between the filters. For each of these inversions, deep and shallow layers have changed significantly, while

around 2000 ms there is not much difference. Radon inversion demonstrates the most change in this area. The blue arrows in this Figure shows the areas where most differences in lateral continuity appear, which happen to lie below the zone of interest. The Radon filter seems to provide the greatest continuty.

# 4. Conclusion

Three different filtering techniques are applied to the data. The data resulting from this process are inverted using simultaneous prestack inversion, and the acoustic impedance results demonstrate that the Radon transform provides the best results. Radon transform is a tool for removing noise, by suppressing the multiples through linearizing the moved out events. Inverse Q enhances certain seismic data, and in some instances may increase the noise present. Bandpass filtering using the frequencies tested here apparently removes some of the lowest frequencies that would have been helpful in maintaining resolution of layers.

The Radon transform is found to be the preferred method of enhancing data quality for inversion in this data set. The Radon transform seems to have particularly improved the results around 2500 ms. The noise in this part of the gather does not seem to be particularly affected by multiples (see Figure 3, for example), although it is treated differently by the three filtering techniques analyzed here. The inverse Q filter appears to have increased that noise, which must have been high frequency, and was amplified by this filter (see Figure 8). On the other hand, the bandpass filter seems to have provided no improvement over the original data at this two-way travel time (see Figure 6,). The conclusion is that the Radon filter has removed incoherent noise and improved the quality of the stack at this two-way travel time.

# 5. References

Ardhuin, F., Lavanant, T., Obrebski, M., Marie, L., Howe, B.M., Lukas, R., and Aucan J., 2013, A numerical model for ocean ultra-low frequency noise: Wave-generated acoustic-gravity and Rayleigh modes: 2013 Acoustical Society of America, 3242–3259 pp.

Feng, H., and Bancroft, J.C., 2006, Avo principles, processing and inversion: Crewes research report, Vol.18.

Li, Y.,Tang. D.,BGP and CNPC, 2005, Background noise identification and q attenuation using point receiver seismic data: Society of Exploration 2005 Annual Meeting, 2205-2208 pp.

Russell, H.B., 1988, Introduction to Seismic Inversion Methods (volume 2): Society of Exploration Geophysicists.

Simm, R., and Bacon, M., 2014, Seismic Amplitude an Interpreter‟s Handbook: Cambridge University.

Tu, N., and Lu, W. K., 2009, Inverse Q filtering to enhance seismic resolution, *2009 IEEE International Geoscience and Remote Sensing Symposium*, Cape Town, 2009, pp. II-345-II-348.

# Appendix A

In this part six different bandpass filter tests applied on the NMO (Normal Move Out) migrated prestack data can be seen. To have a better understanding on the filtering process, the original data, the filtered data, and the rejected parts are shown respectively in the following Figures. For bandpass filter test1, test2, and test3, it can be said that the filters have the tendency to remove meaningful data from the original seismic data while bandpass tests 4 and 6 fail to remove enough noise from the seismic without altering the original data. Bandpass test 5 is chosen as the preferred filter, because it removes the noise, and do not alter the important data in the area of research (Figure 25). Bandpass-5 may not be the optimum filter for removing noise, but it does not remove important gathers from the seismic while removing the noise. It improves signal over noise ratio without lowering signal quality. That is why bandpass-5 is chosen to be the preferred bandpass filter applying inversion.

# Appendix B

In this part, four different Inverse Q filtering are applied to the entire prestack data are shown. However, for the purpose of better comparisons the Figures show one inline (1177) passing through well L-30. Each figure shows NMO migrated prestack data, Inverse Q filtered data, and the added frequencies data in order to apply inverse Q to the data respectively. In inverse Q, not adding too much extra information to the data in order to improve the quality is important. Comparing following Figures (Figure 27, Figure 28, Figure 29, and Figure 30) it can be said that the inverse Q test 2 and test 3 added enormous amount of unwanted traces to the data. These redundant traces disrupt the data and distort the quality of seismic image. In tests 1 and 4 it can be seen that the inverse Q processes distorted the original data. Less values for Q 600 it is observed that there is not a significant change for the data. However, there are still minor changes can affect the seismic data. That is why, Q 600 is taken as the

preferred quality factor. In the Figure 27 the inverse Q filtered data with the 600 quality factor can be seen as the preferred filter for inverse Q.

# Appendix C

In this section Radon transform tests are compared. Four different test are executed in order to compare them to each other and decide the optimum Radon transform for further investigations. The following Figures (Figure 31,32,33, and 34) show the original prestack seismic data, the Radon filtered data, and the rejected part after Radon transform respectively. For the first three tests it can be said that, there are no major differences between them, at first sight. However, if examined closely the selected area, Radon-2 and Radon-3 remove more data than intended. Radon-1 removes noise consistently while keeping the necessary traces in the seismic. In this case Radon transform test-1 improves signal identifying primaries while removing most of the multiples. Furthermore Radon-1 is chosen to be the preferred Radon transform for this study.

# Figures

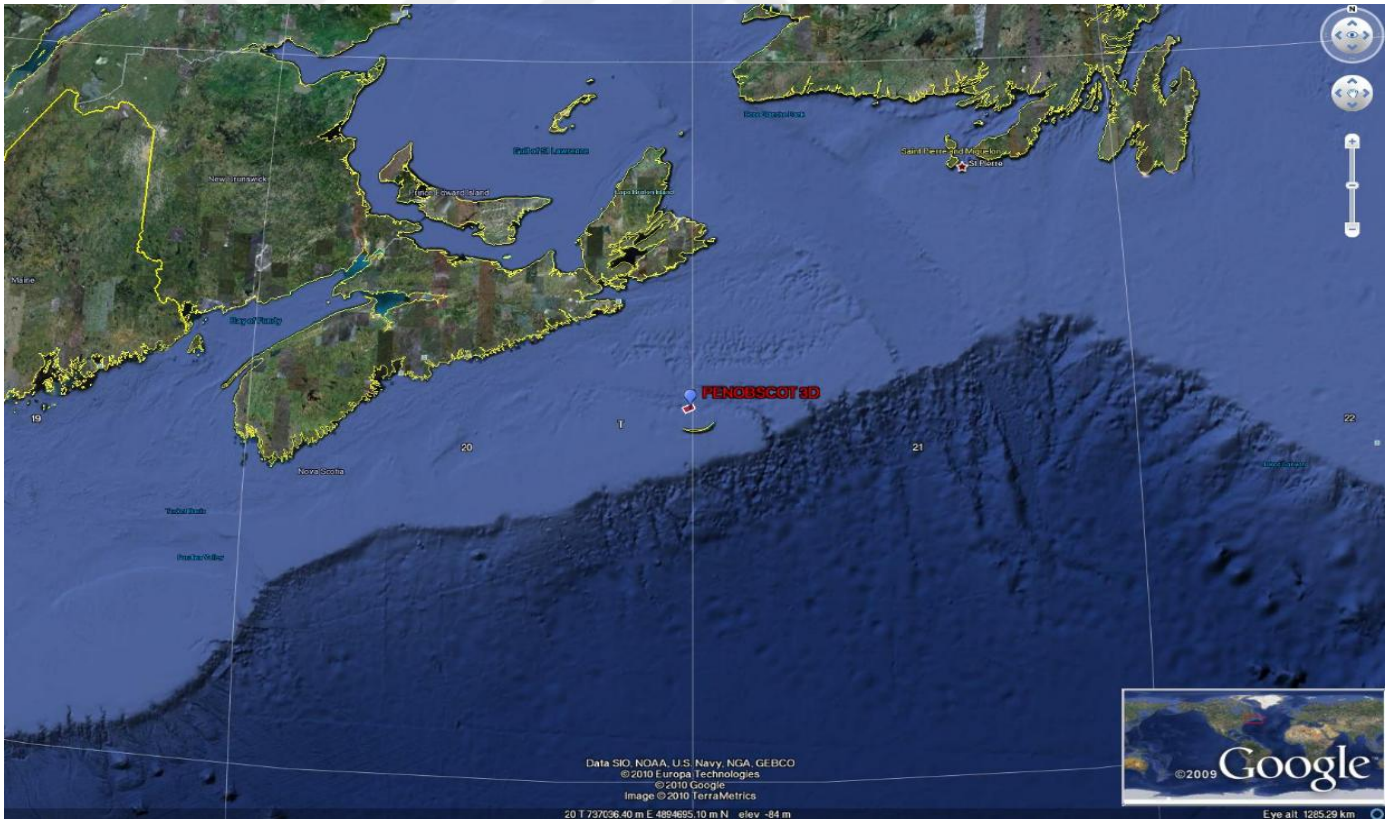


Figure 1: Map of offshore eastern Canada. The area where the seismic data used in this study is shown by the blue dot offshore of Nova Scotia (modified from Google Earth, ©2016 Google Image Landsat) (used with permission, documentation seen on page 54).

Table 1: Seismic data acquisition parameters

| | | |
|---|---|---|
| Inline Range | 1000 | 1600 |
| Crossline Range | 1000 | 1481 |
| Basin Size (m) | 12.01 | 25.01 |
| Z Range (ms) | 0 | 6000 |
| Size (km) | 7.2*12.03 | |
| Total Number of Gathers | 19280 | |

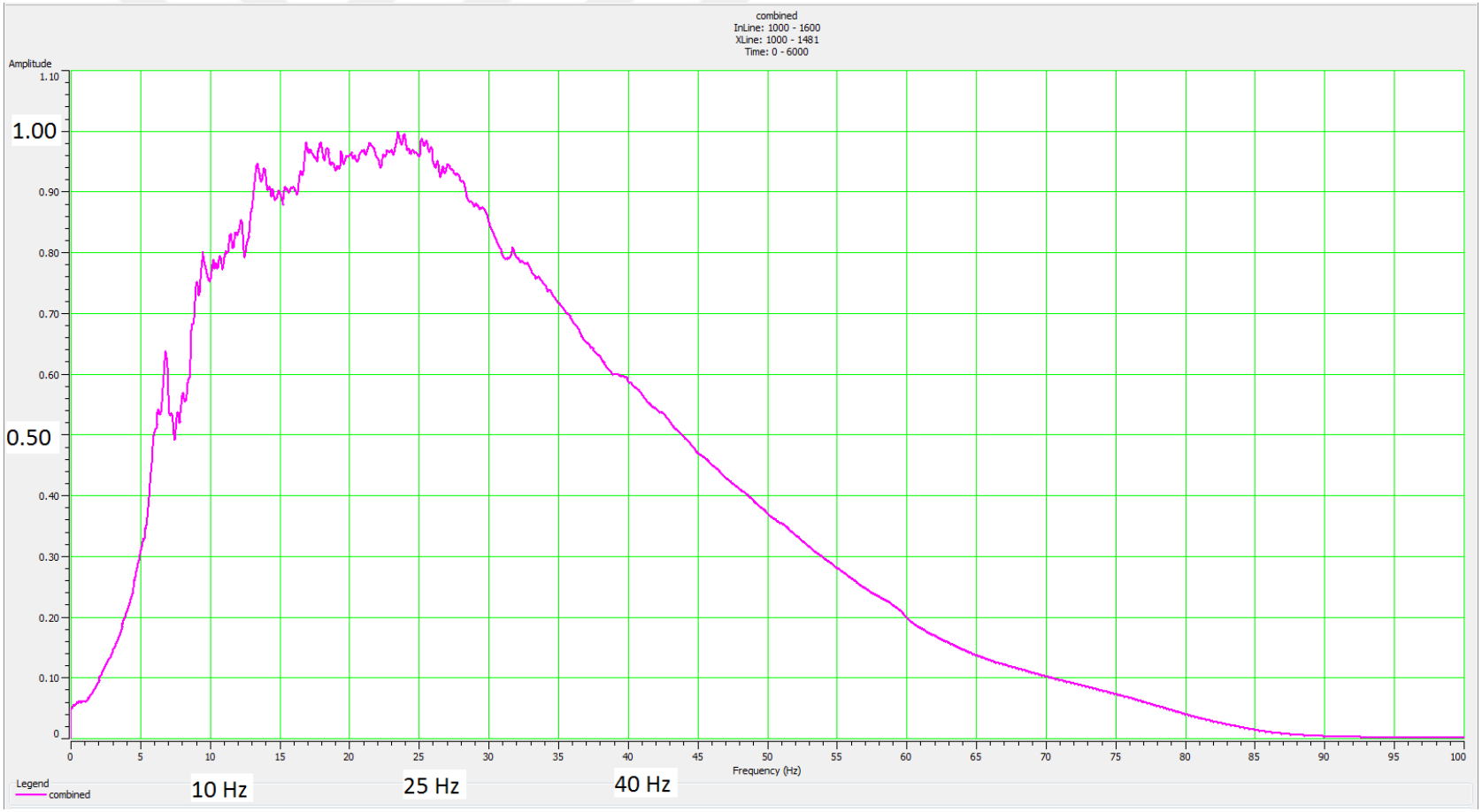


Figure 2: Normalized amplitude spectrum of the original prestack data for the entire seismic volume.

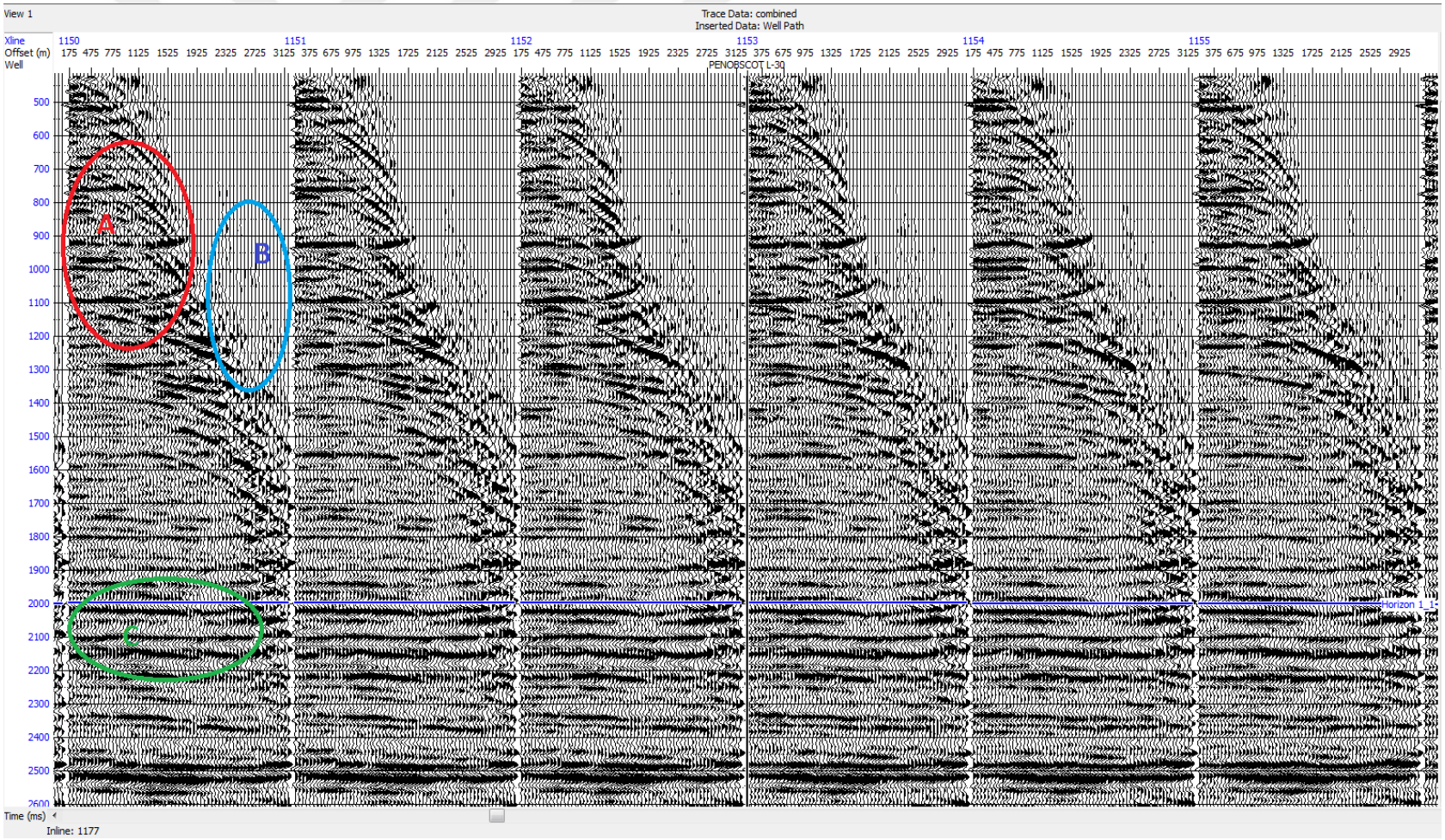


Figure 3: NMO corrected six gathers for the seismic prestack data, time here is 500-2500 ms, for inline 1177. The circled area labeled A shows the multiples and shallow noise in the seismic gather, B shows the noise, and C shows the real reflections.

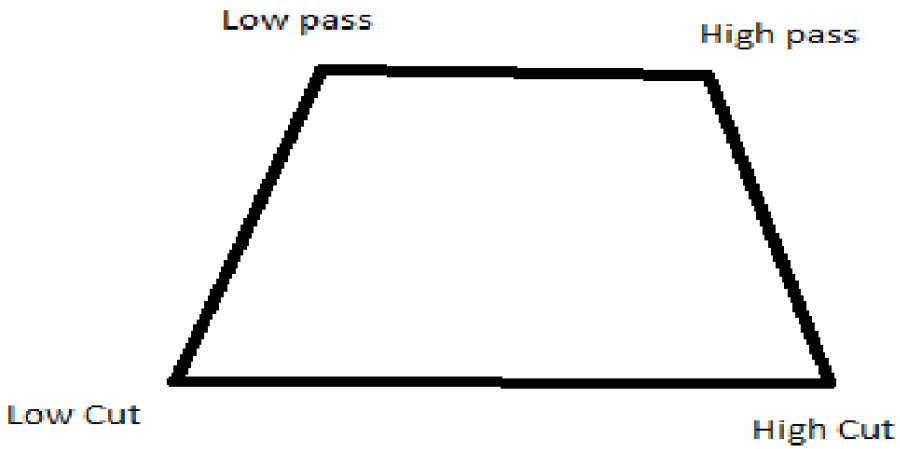


Figure 4: Bandpass filter frequency intervals, inside of these intervals different frequency values pass.

Table 2: Bandpass filter parameters for the various tests

| | Low Cut | Low Pass | High Pass | High Cut |
|---|---|---|---|---|
| Bandpass-1 | 5 | 10 | 50 | 80 |
| Bandpass-2 | 0 | 5 | 10 | 15 |
| Bandpass-3 | 10 | 15 | 40 | 70 |
| Bandpass-4 | 5 | 15 | 30 | 40 |
| Bandpass-5 | 1 | 8 | 40 | 70 |
| Bandpass-6 | 5 | 10 | 40 | 70 |

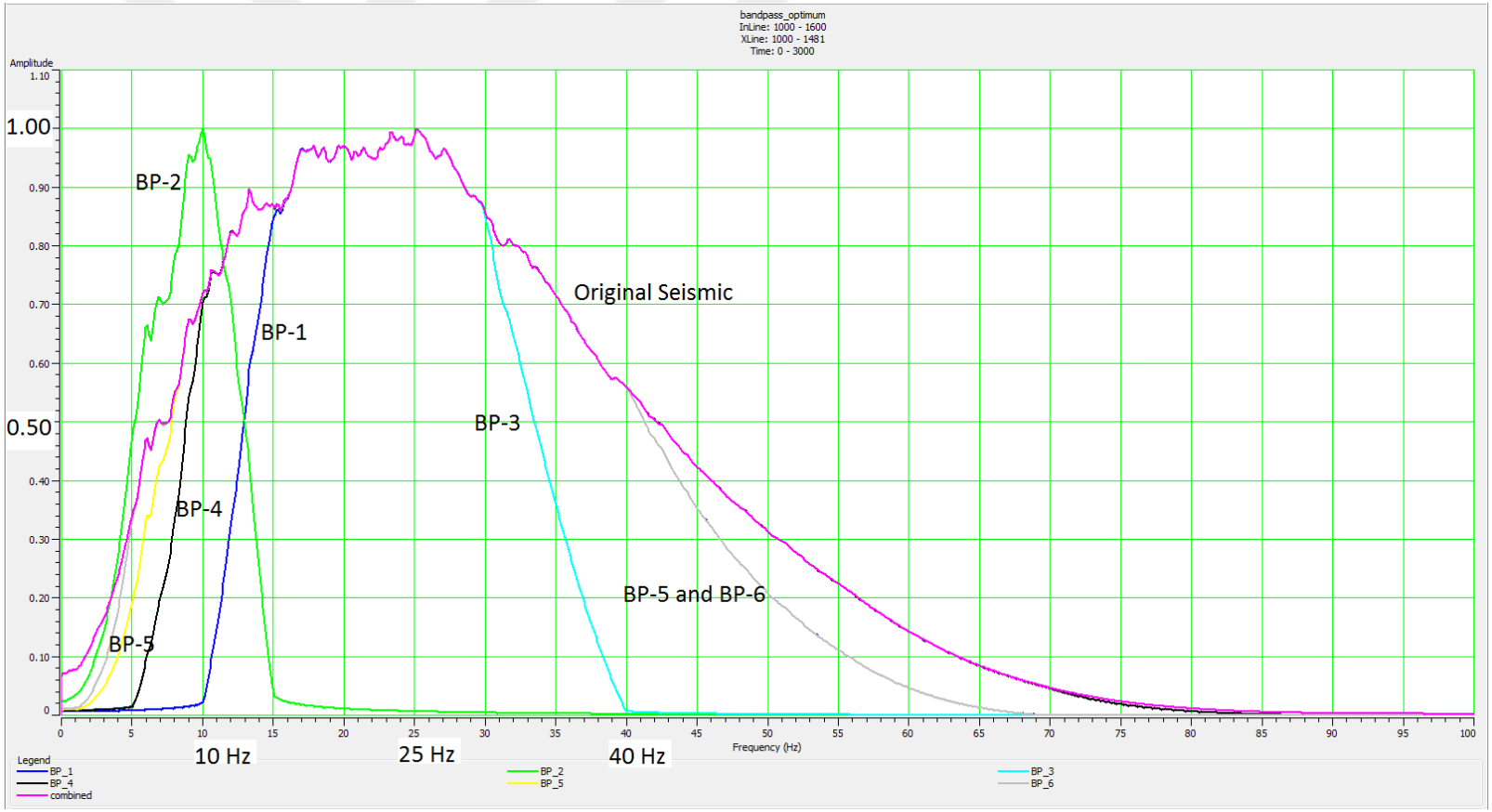


Figure 5: Amplitude spectrum comparison for Bandpass Filtering. BP-5 is applied to the data as the optimum filter for our data interval values. The amplitude spectrum of BP-6 overlaps the BP-5 after 40 Hz. The grey color shows both BP-5 and BP-6 after 40 Hz. Each spectrum covers the entire seismic data volume.

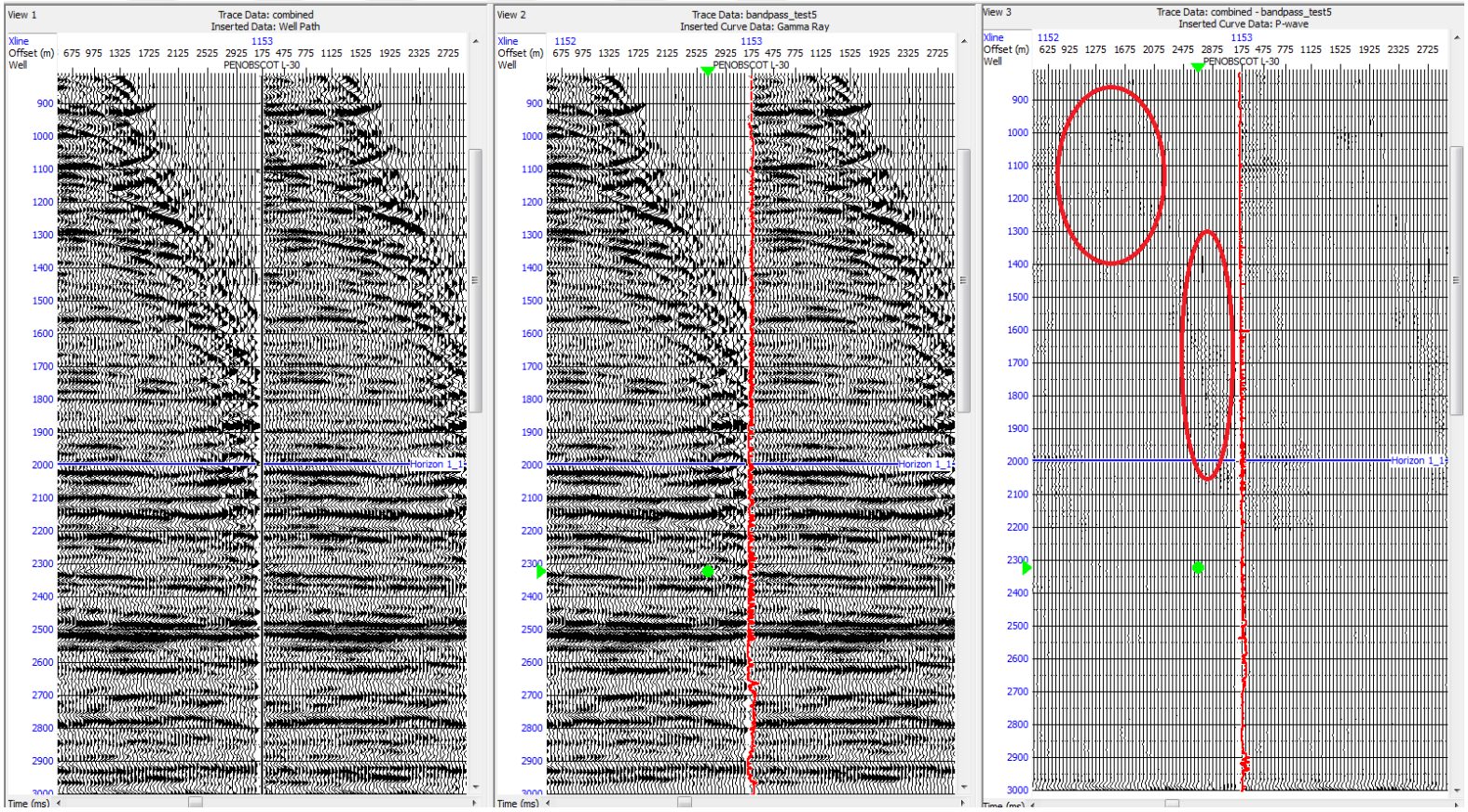


Figure 6: The effect of bandpass filtering for the preferred filter Bandpass-5. In this and similar subsequent images, the gathers on the left show the original data, in the middle the filtered data, and on the right the difference. 900-3000ms shown. Red circles show multiples and noise.

Table 3: Inverse Q parameters for the various tests.

| | Constant Q |
|---|---|
| Inverse Q-1 | 600 |
| Inverse Q-2 | 200 |
| Inverse Q-3 | 300 |
| Inverse Q-4 | 800 |
| Inverse Q-5 | 400 |

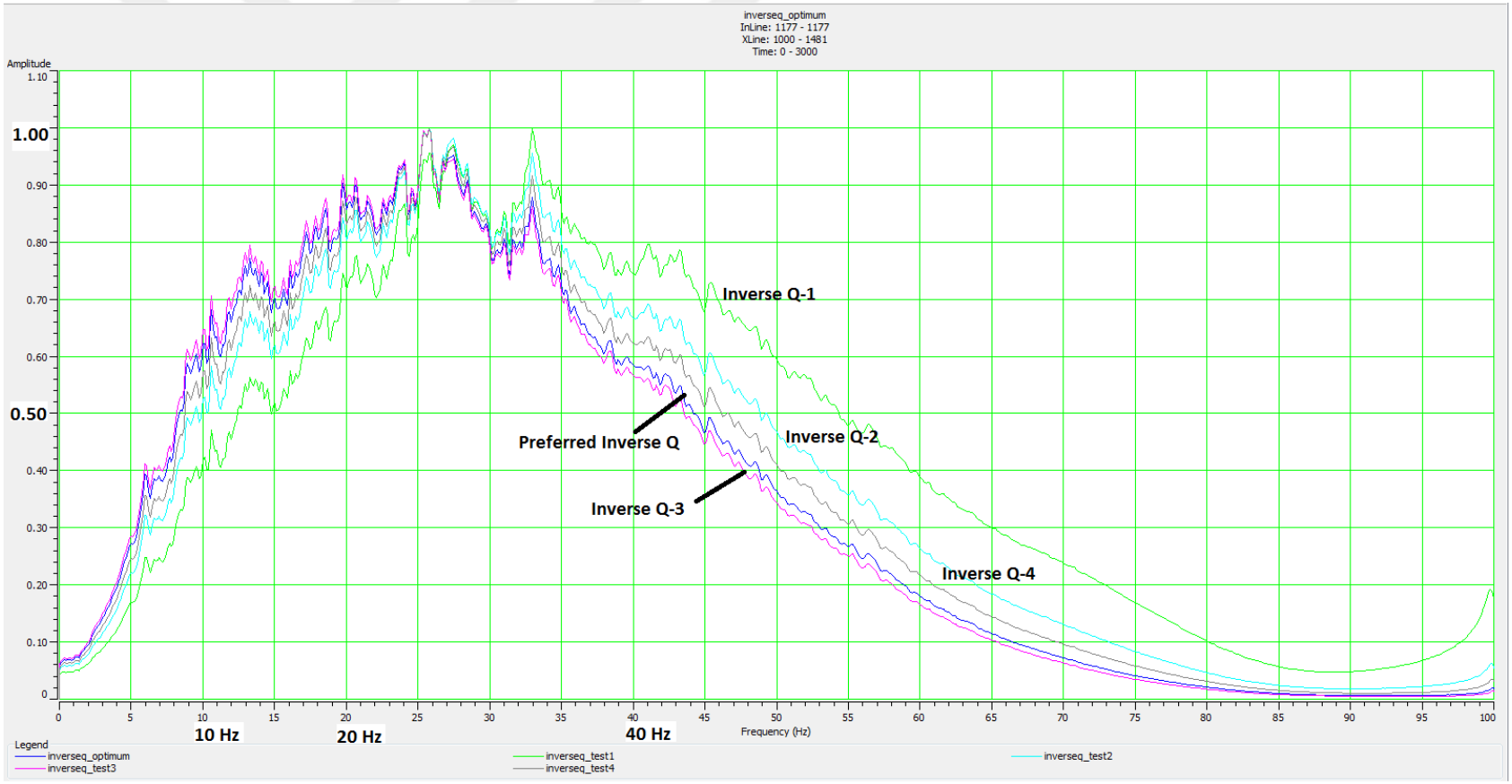


Figure 7: Normalized Inverse Q amplitude spectrum for all tests, including the entire volume.

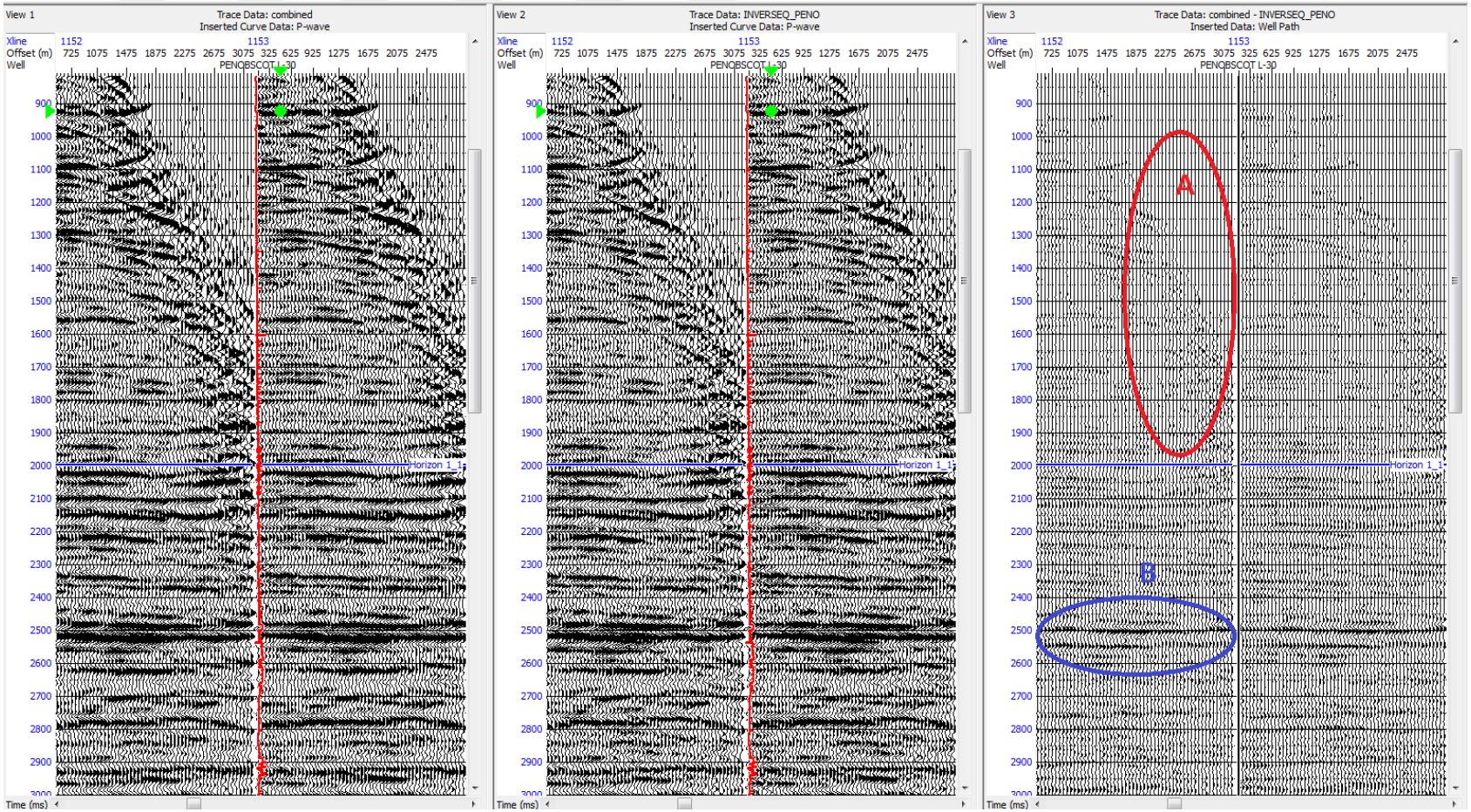


Figure 8: The effect of Inverse Q filtering for the preferred filter, Q-1. A shows added multiples and noise, while B shows added extra information in order to improve the signal.

Table 4: Radon transform parameters for the various tests.

| | High Delta (ms) | Low Delta (ms) |
|---|---|---|
| Radon-1 | 160 | -160 |
| Radon-2 | 100 | -100 |
| Radon-3 | 200 | -200 |
| Radon-4 | 1000 | -1000 |

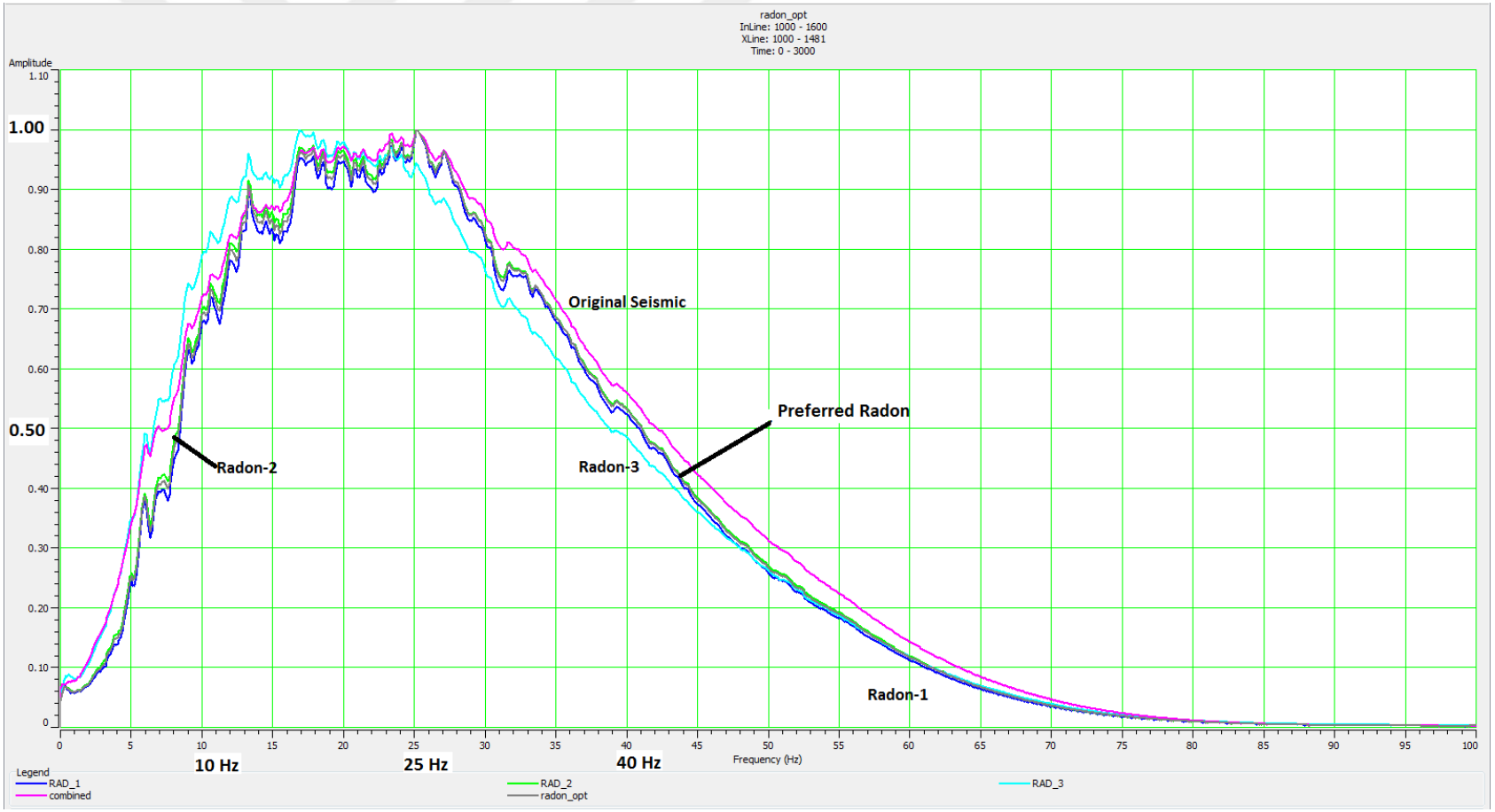


Figure 9: Radon Transform Amplitude Spectrum Comparison for all tests, including the entire seismic volume.

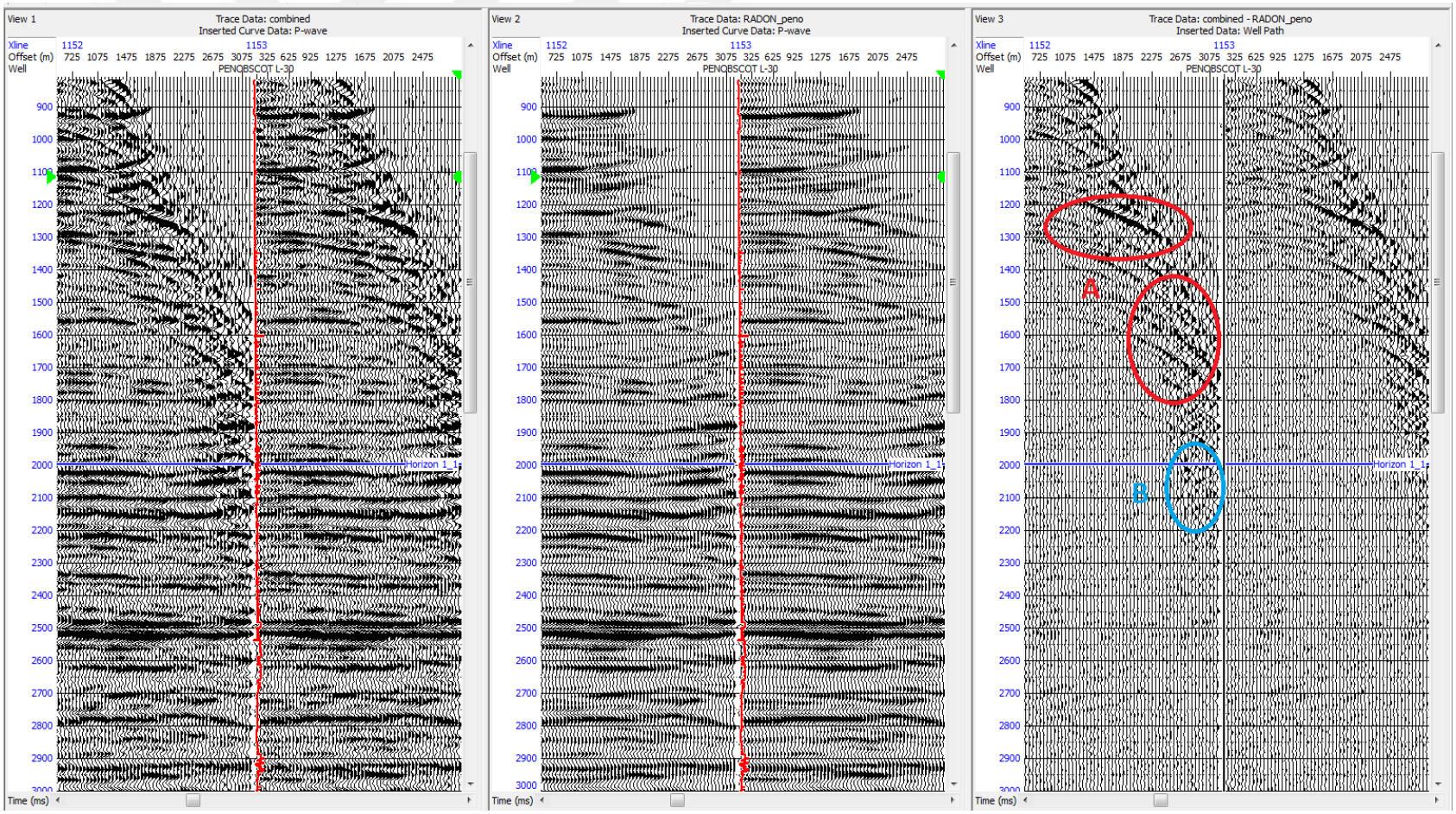


Figure 10: The effect of Radon filtering for the preferred filter Radon-1. A shows the multiples and noise rejected, while B shows real reflections rejected.

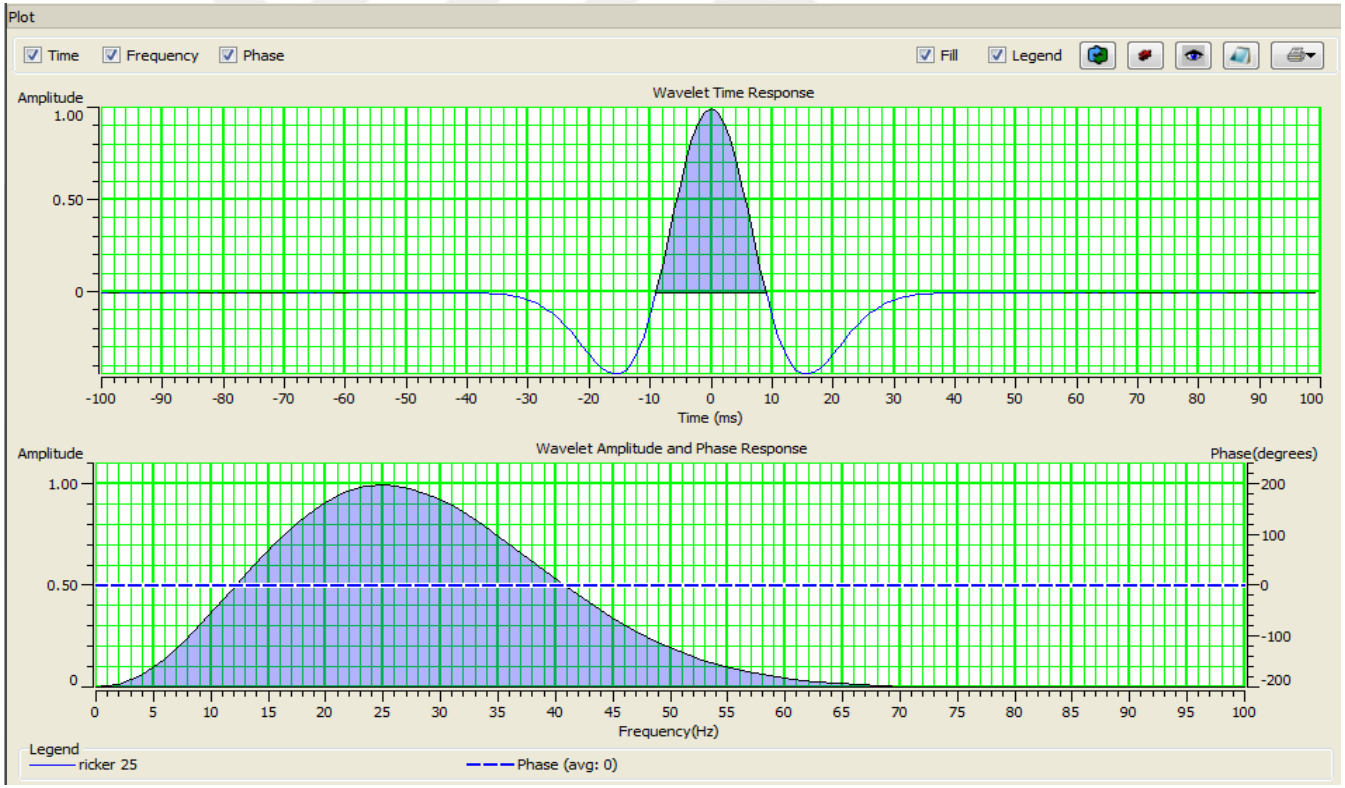


Figure 11: 25 Hz Ricker wavelet and its spectrum.

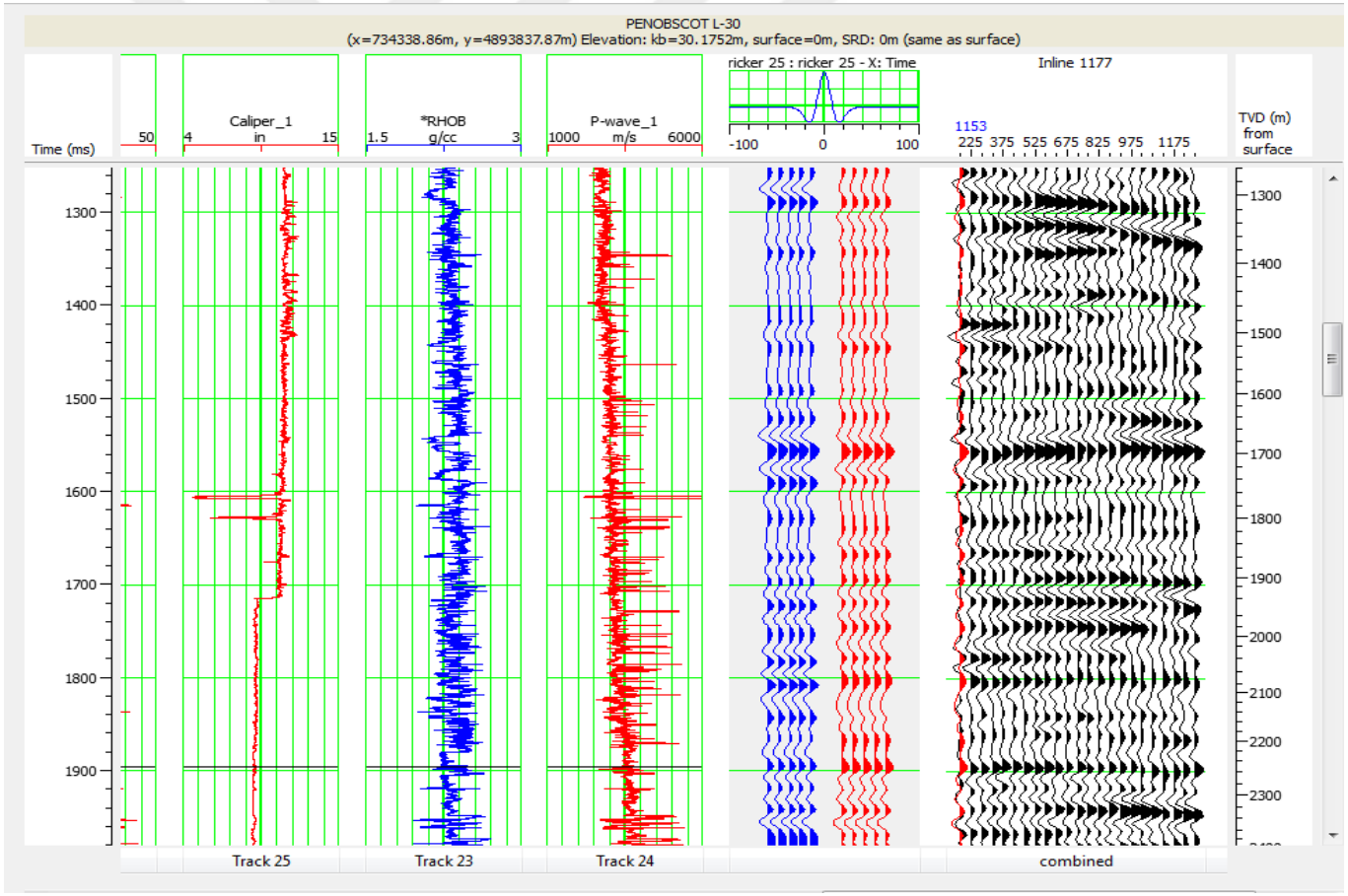


Figure 12: Well tie. The blue trace shows the synthetic seismogram generated from density and sonic logs with 25 Hz Ricker wavelet, and the red trace shows the original seismic. The correlation between synthetic and the original seismic is 0.71.

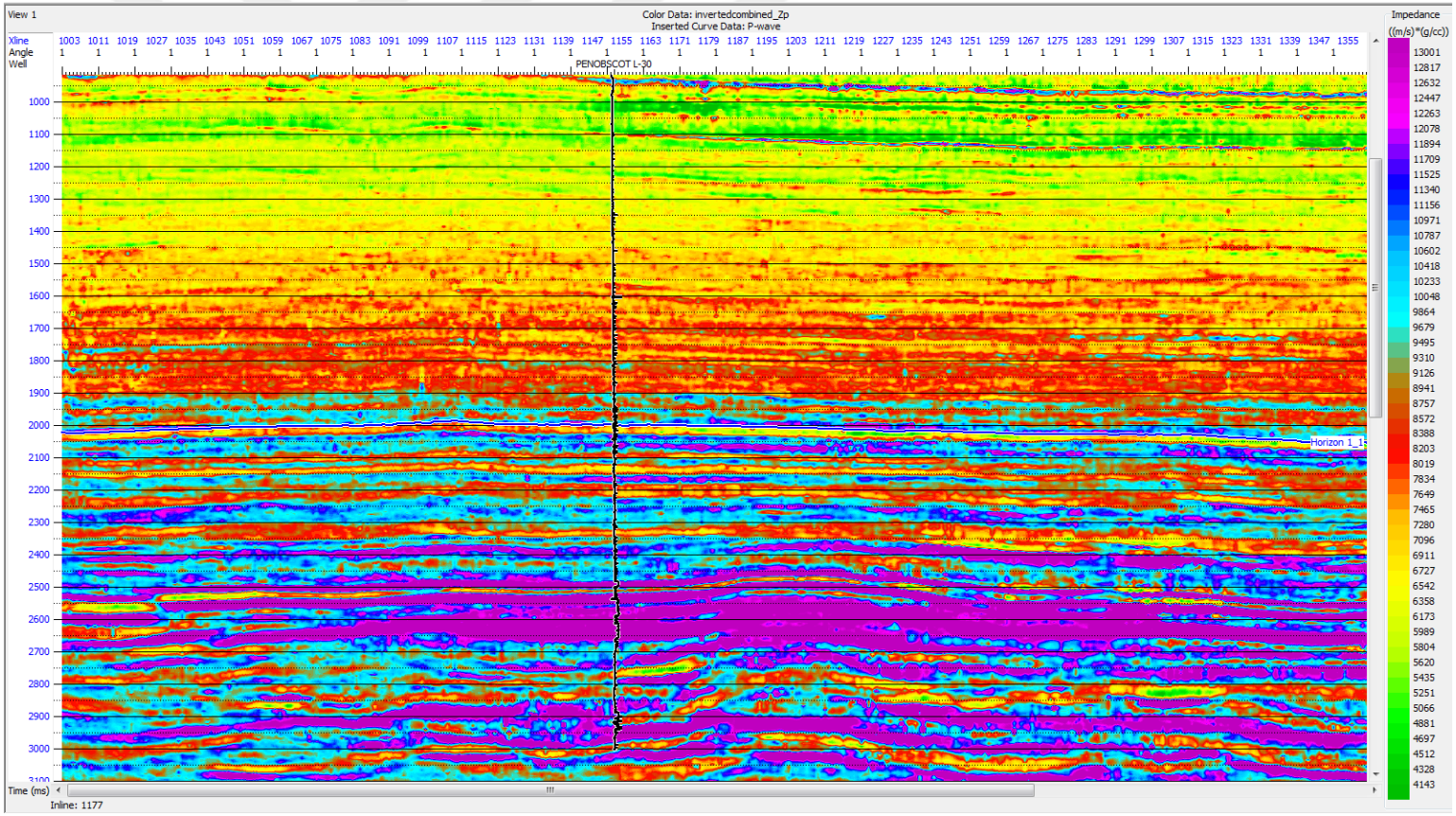


Figure 13: Simultaneous inversion result for Zp from the original seismic data for inline 1171, and time 1000-3000 ms.

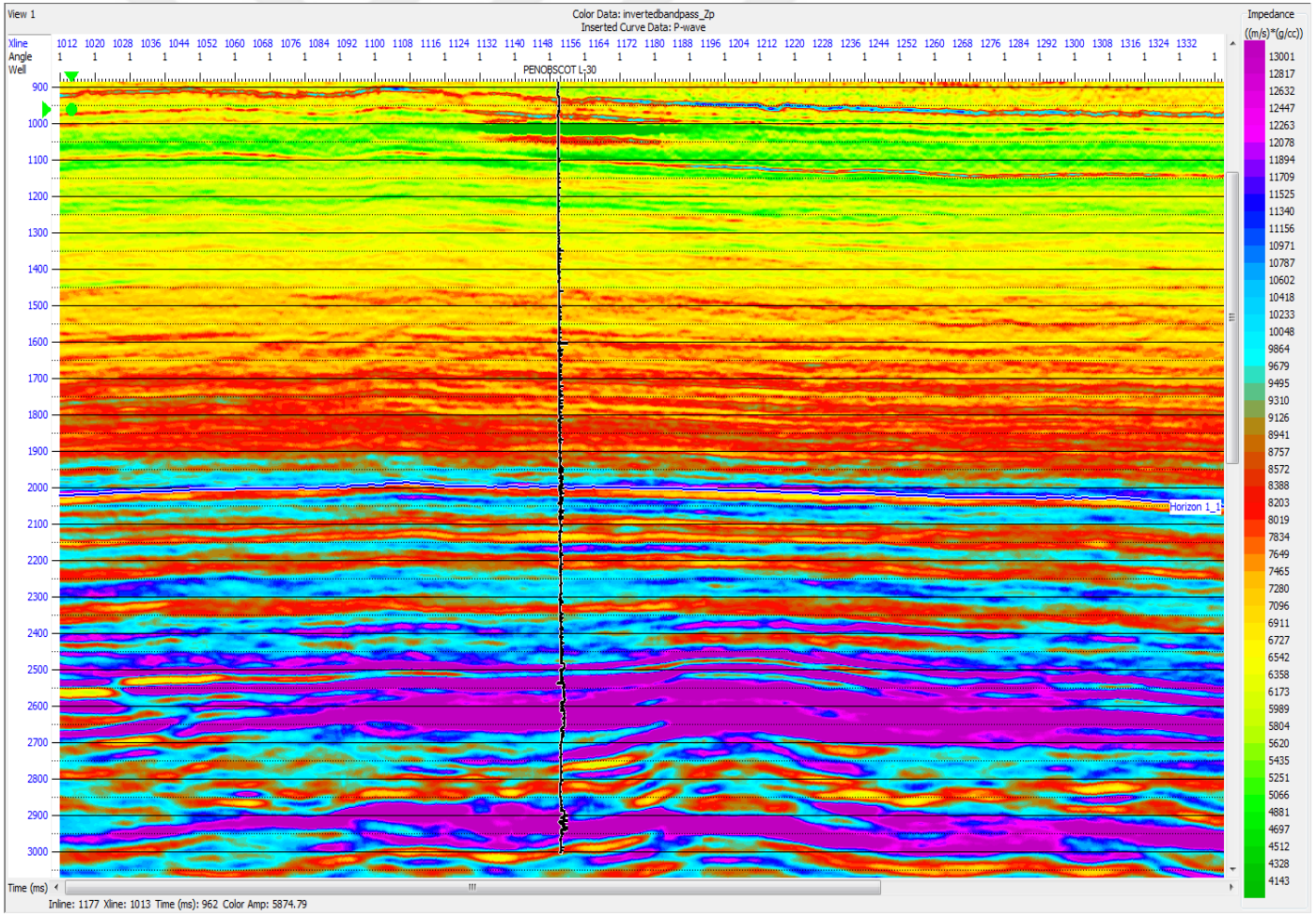


Figure 14: Simultaneous inversion result for bandpass filter (BP-5) for inline 1171, and time 1000-3000 ms.

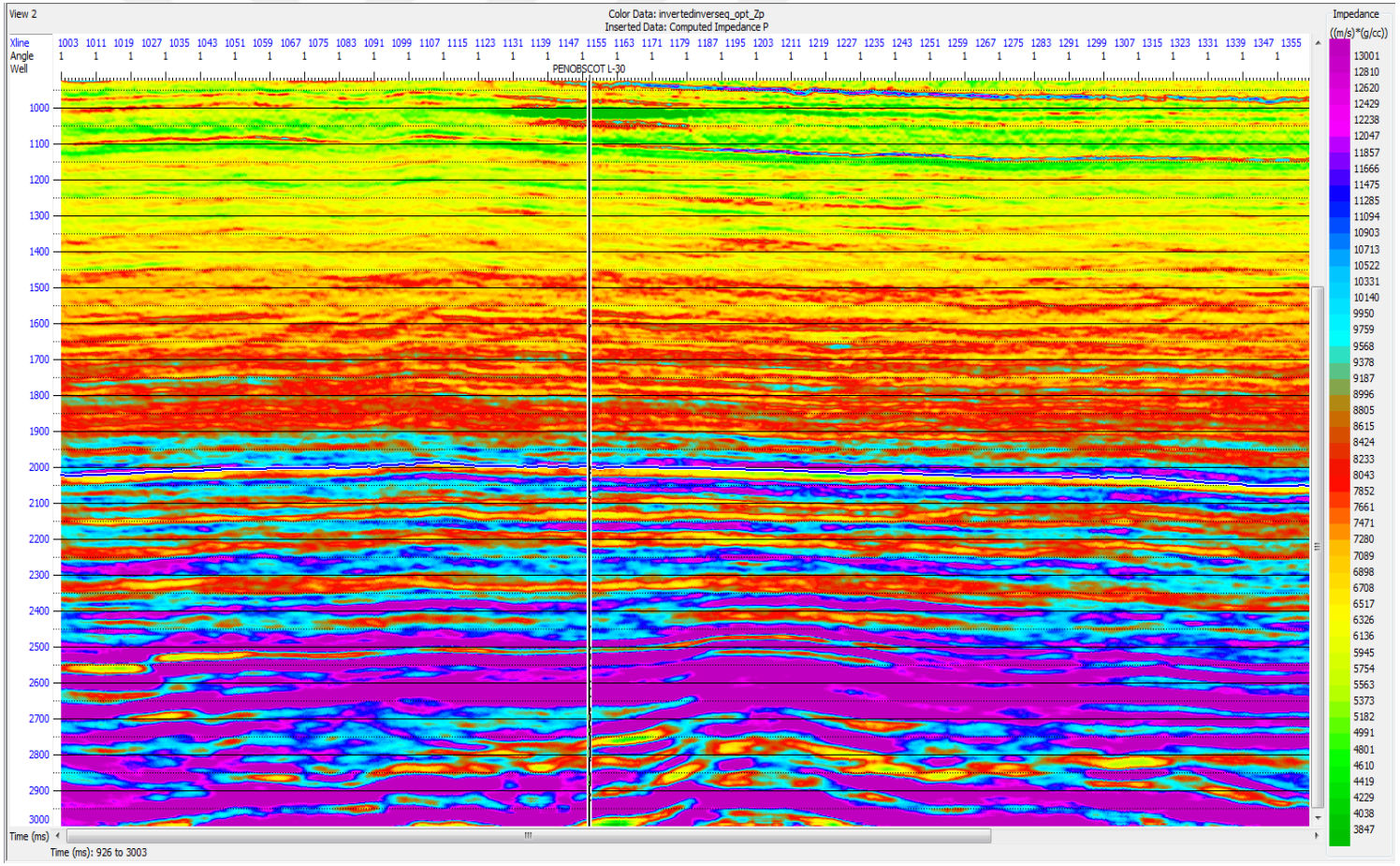


Figure 15: Simultaneous inversion result for inverse Q filter for inline 1171, and time 1000-3000 ms.

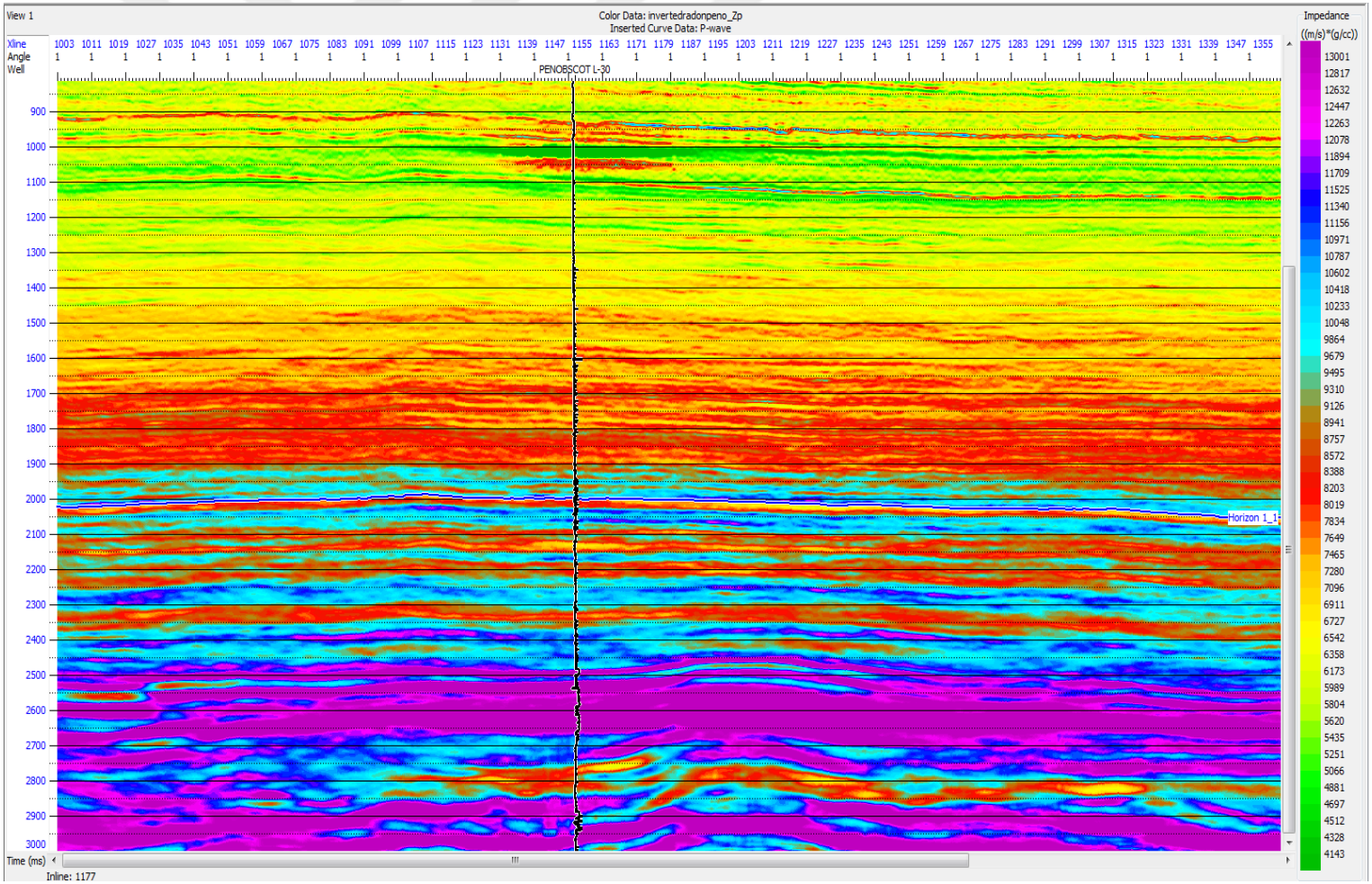


Figure 16: Simultaneous inversion result for Radon transform for inline 1171, and time between 1000 to 3000 ms.

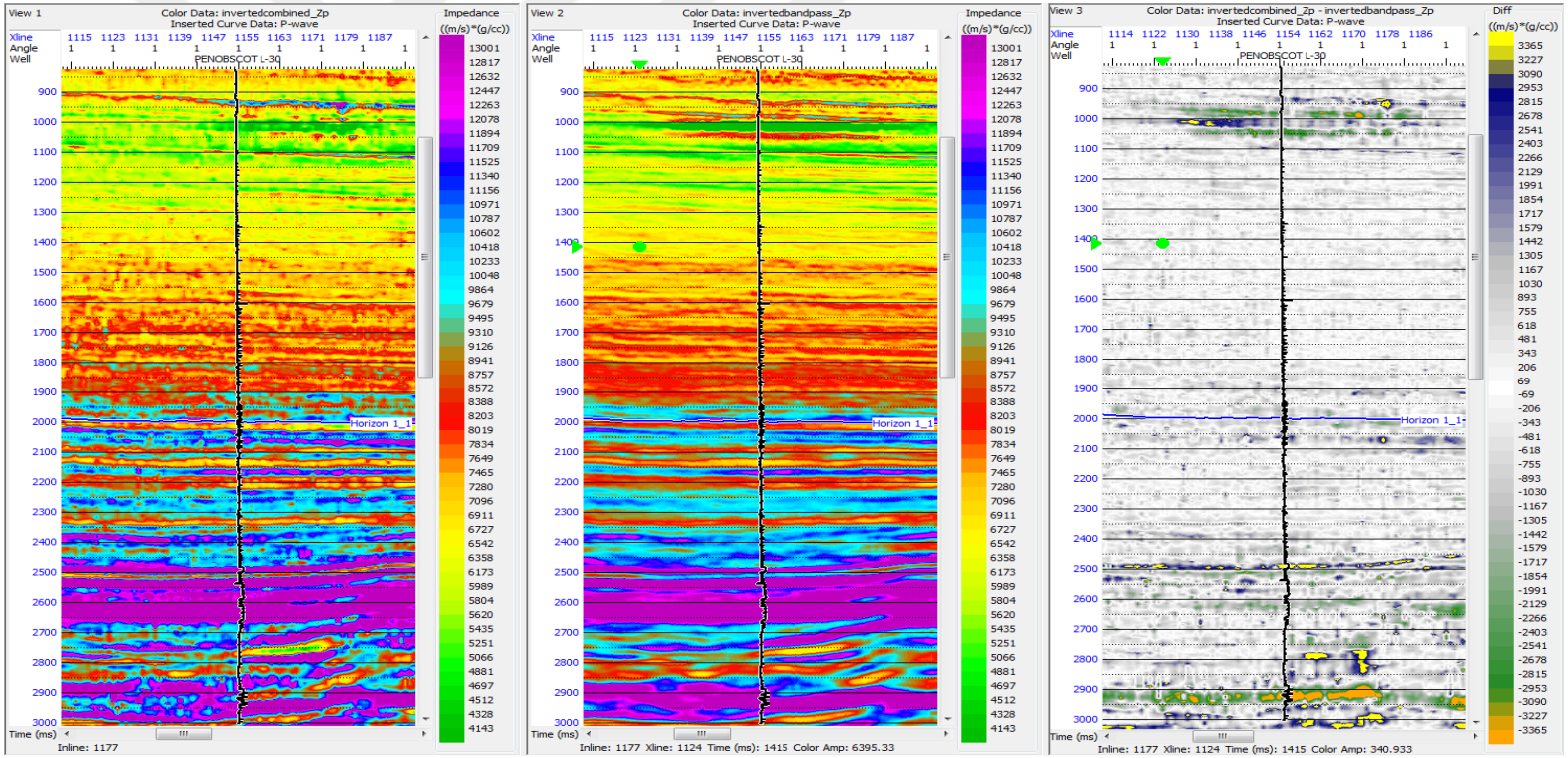


Figure 17: Inversion result for the original seismic (left), bandpass-filter inversion results (middle display), and differences between the two (right side) for inline 1171, 1000-3000 ms.

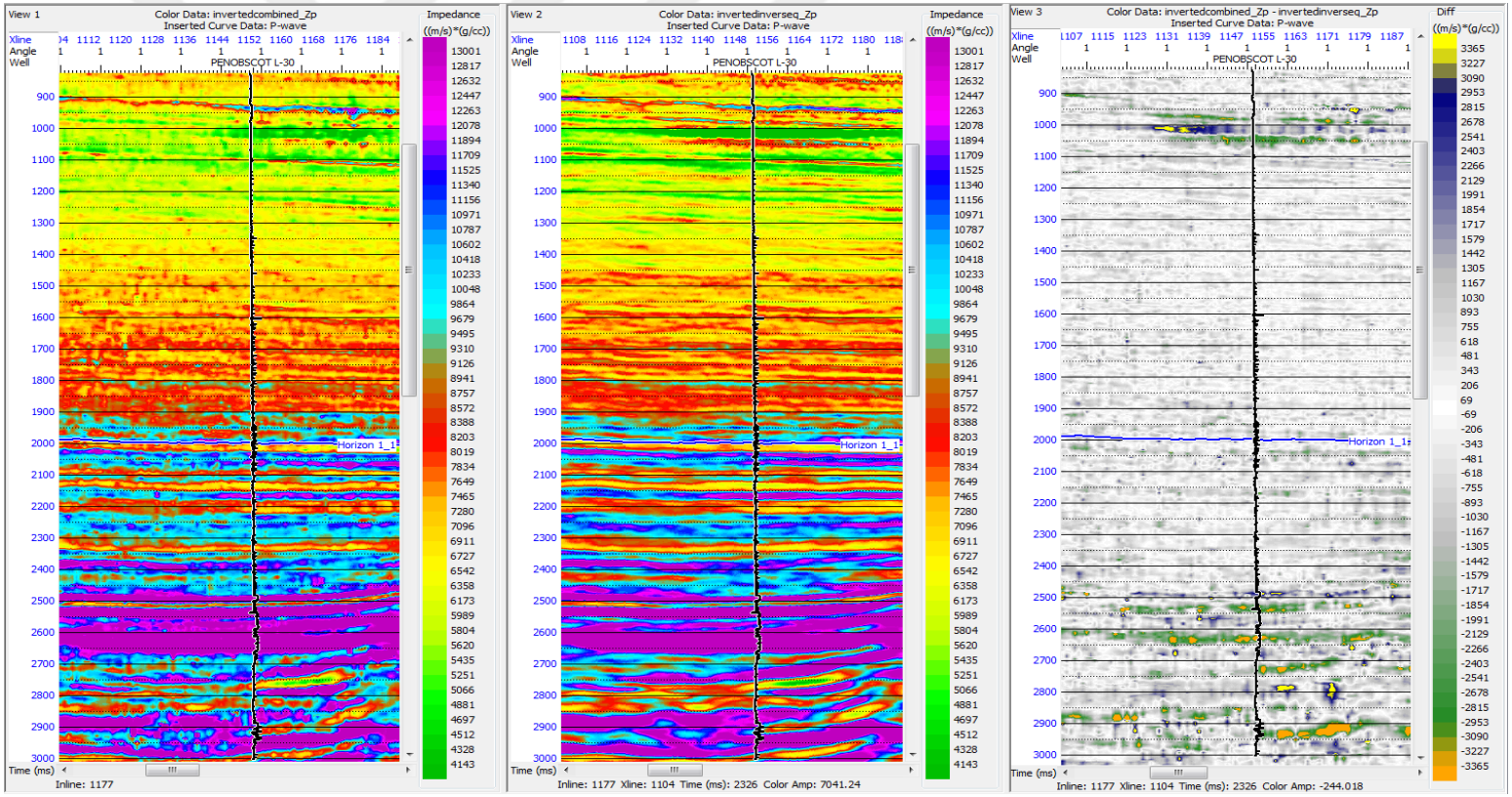


Figure 18: Inversion result for the original seismic (left), inverse-Q inversion results (middle display), and differences between the two (right side) for inline 1171, 1000-3000 ms.

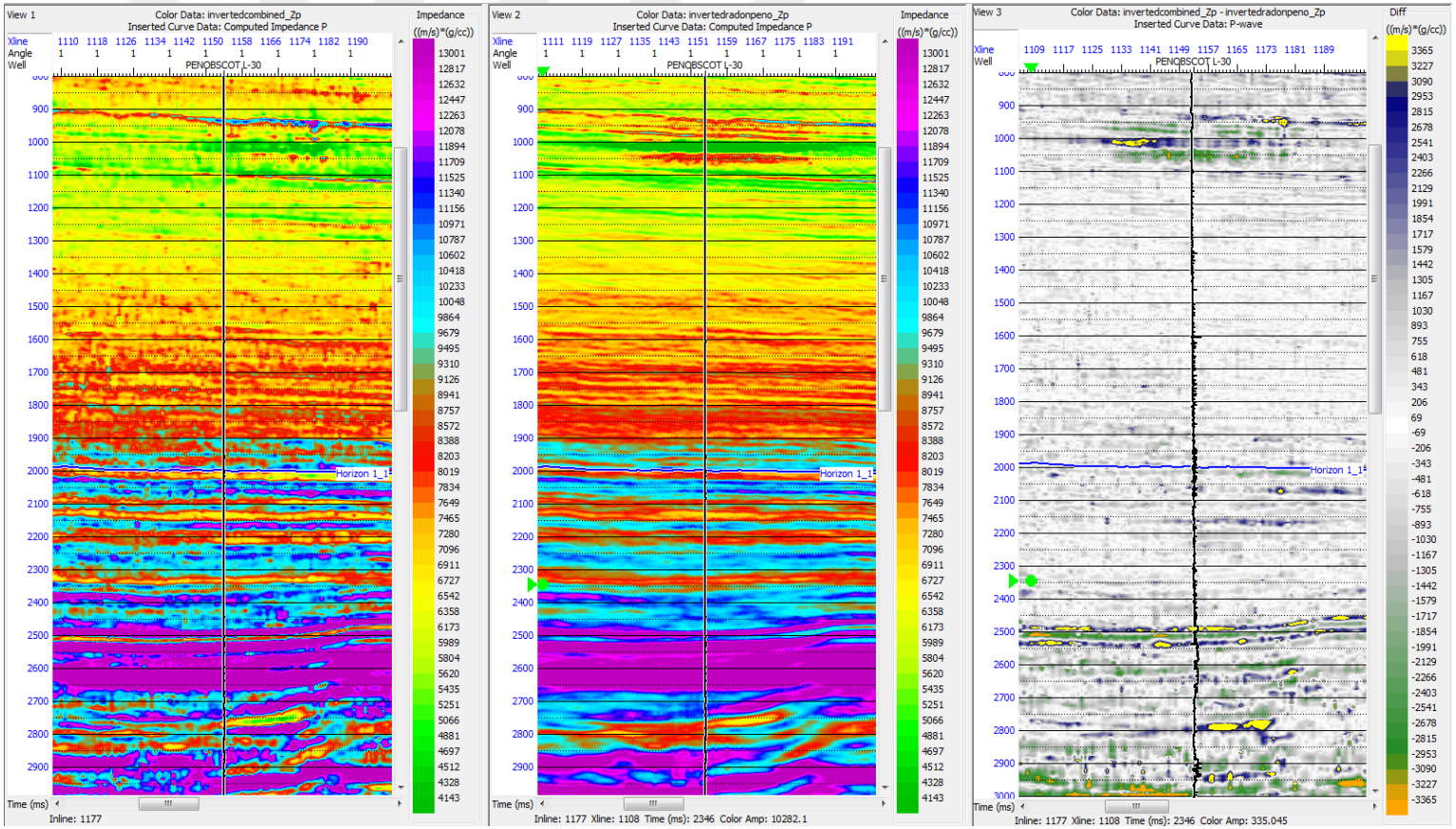


Figure 19: Inversion result for the original seismic (left), radon-filter inversion results (middle display), and differences between the two (right side) for inline 1171, 1000-3000 ms.

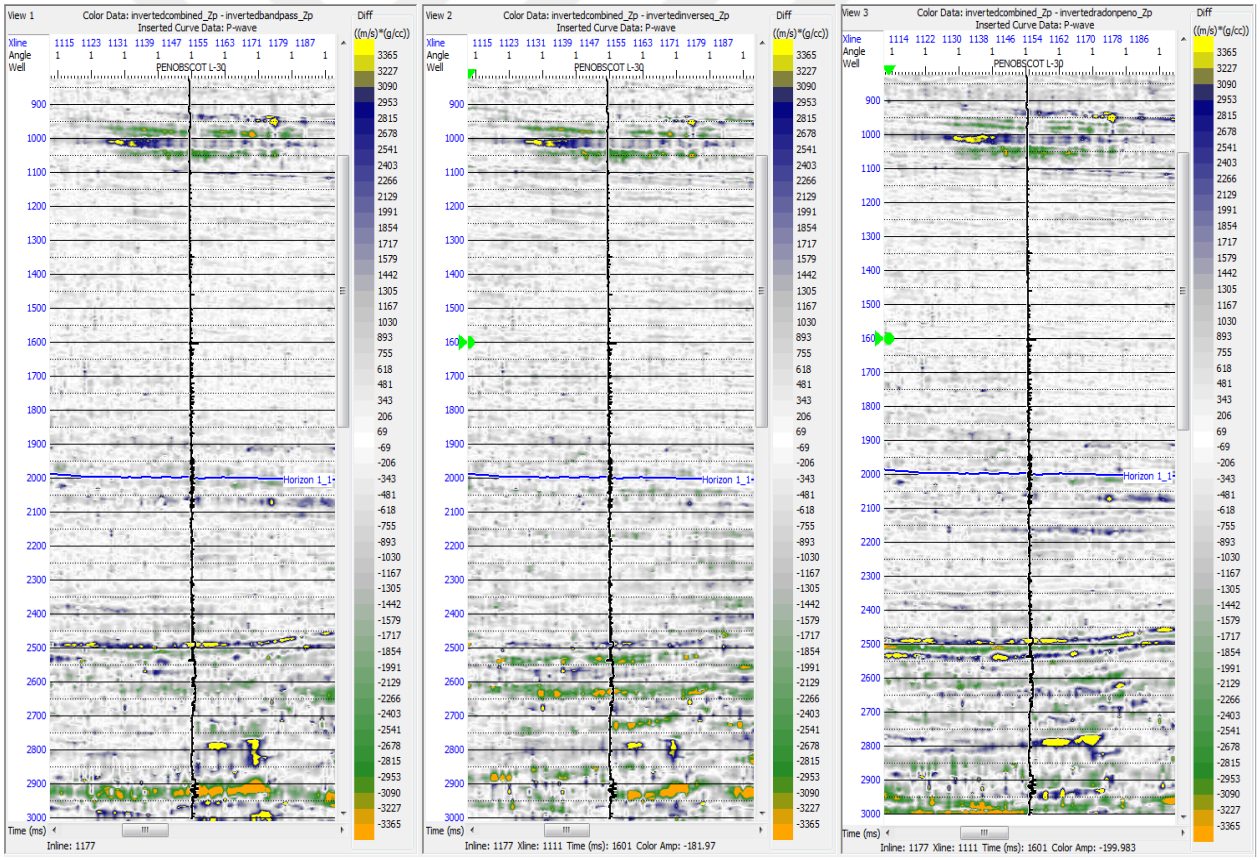


Figure 20: Comparison of the inversion differences. Left to right: the difference between the original data and the bandpass filter inversion, the original data and the inverse Q filter inversion, and the original data and the radon transform inversions. Blue arrows show the areas of most difference of lateral continuity among the three versions.

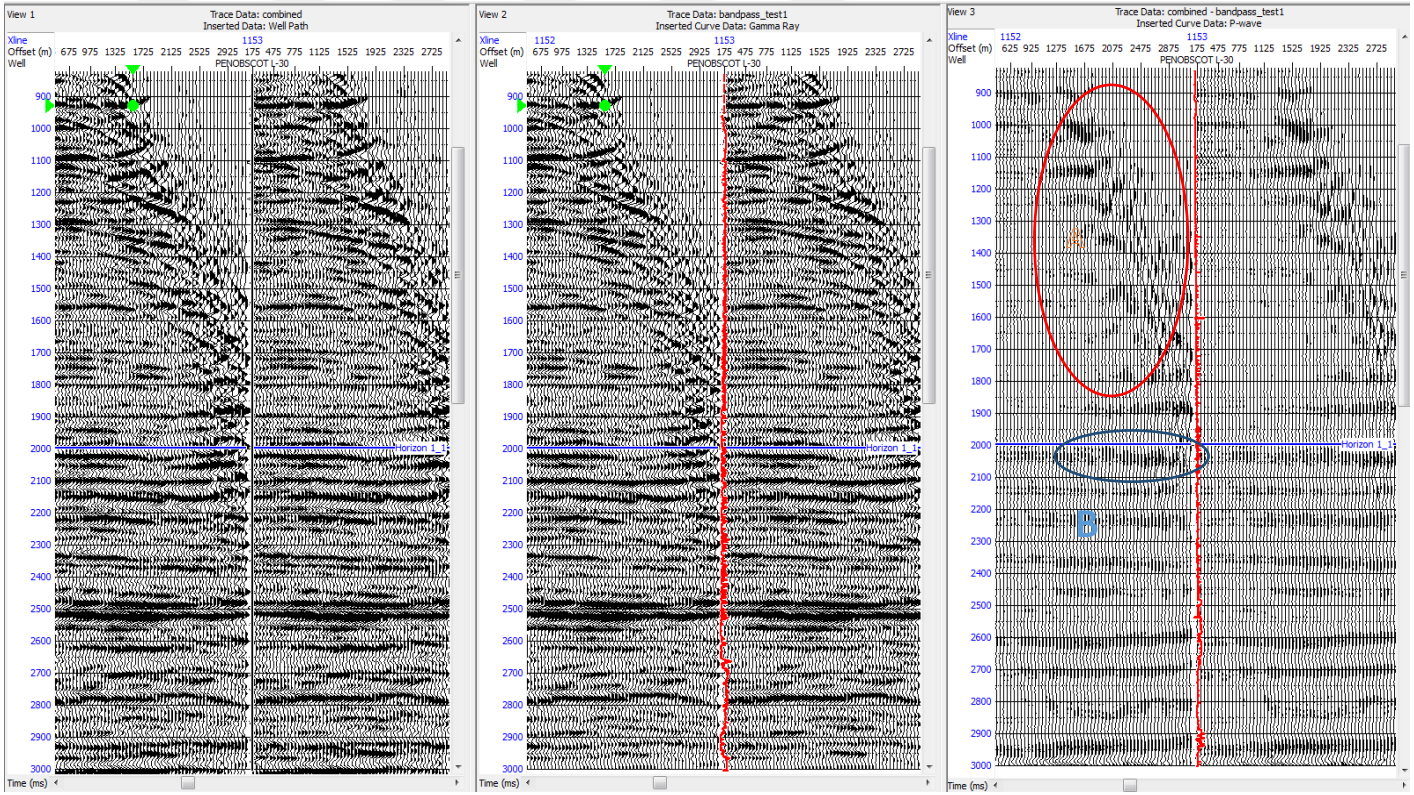


Figure 21: Bandpass filter test1. Original prestack data, bandpass filtered data, and the rejected part of the data are shown respectively for Inline 1177 and crossline 1153. A shows the multiples and noise rejected, while B shows rejected real reflections.

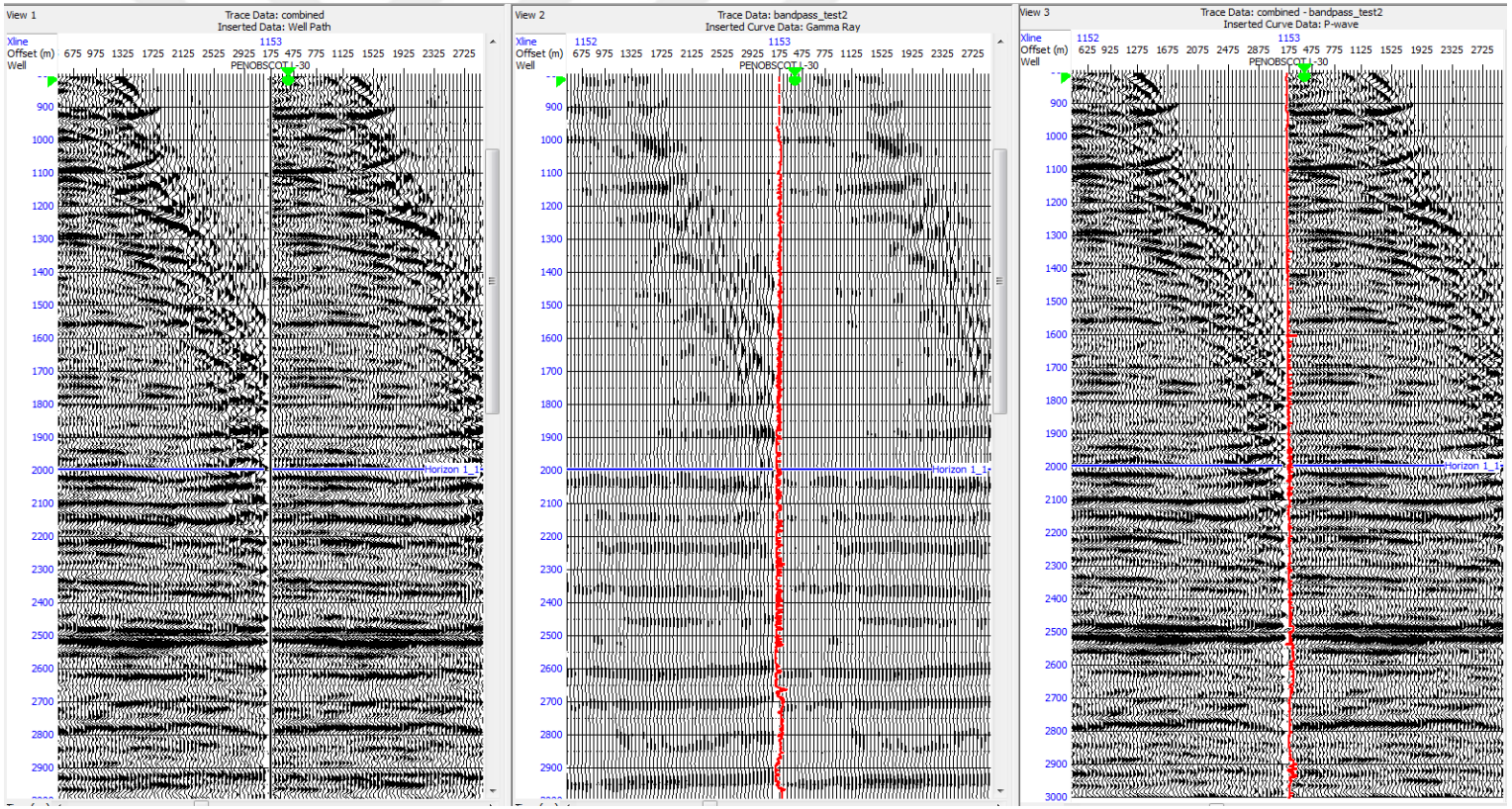


Figure 22: Bandpass filter test 2. Original prestack data, bandpass filtered data, and the rejected part of the data are shown respectively for Inline 1177 and crossline 1153.

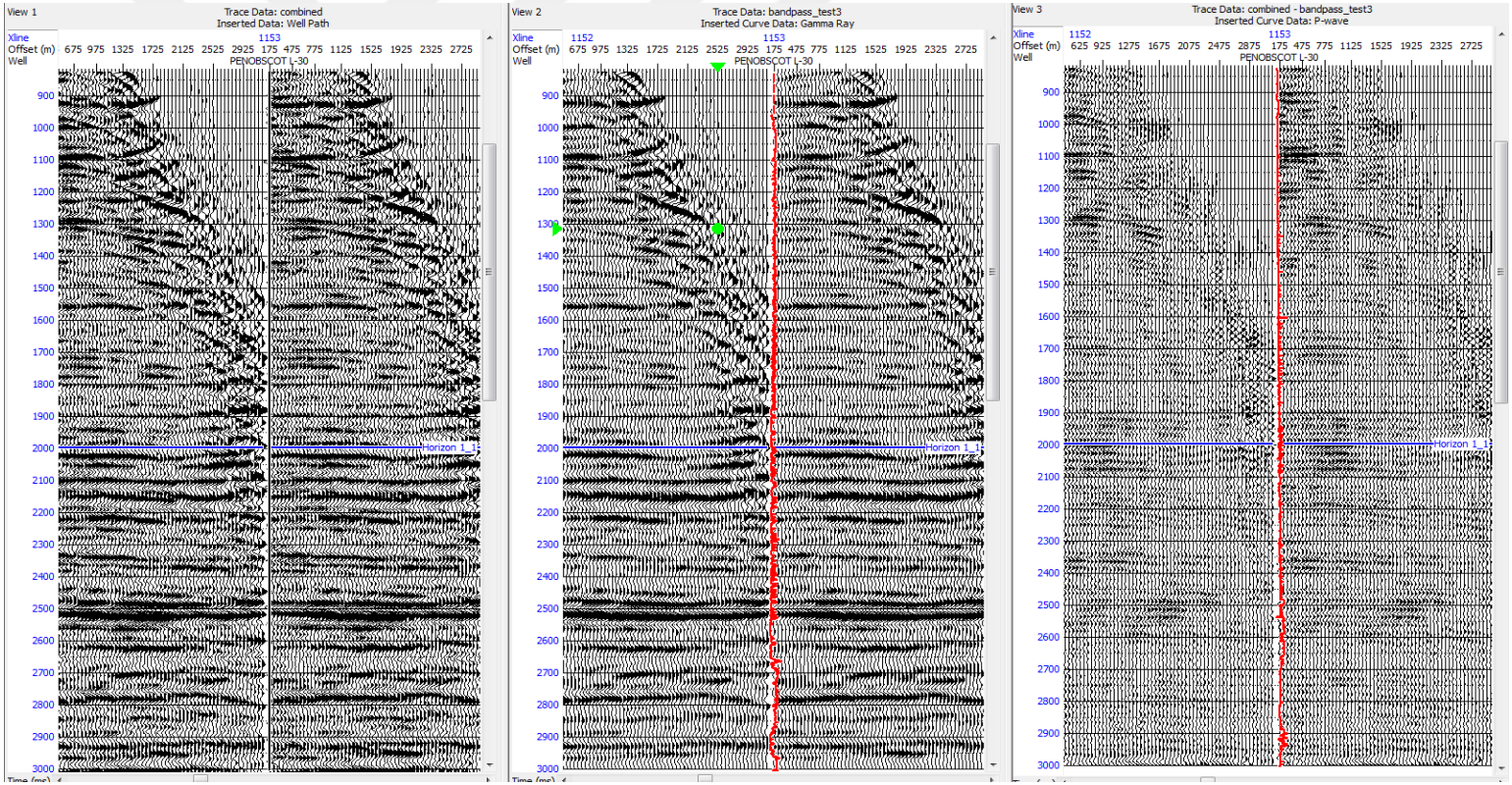


Figure 23: Bandpass filter test 3. Original prestack data, bandpass filtered data, and the rejected part of the data are shown respectively for Inline 1177 and crossline 1153.

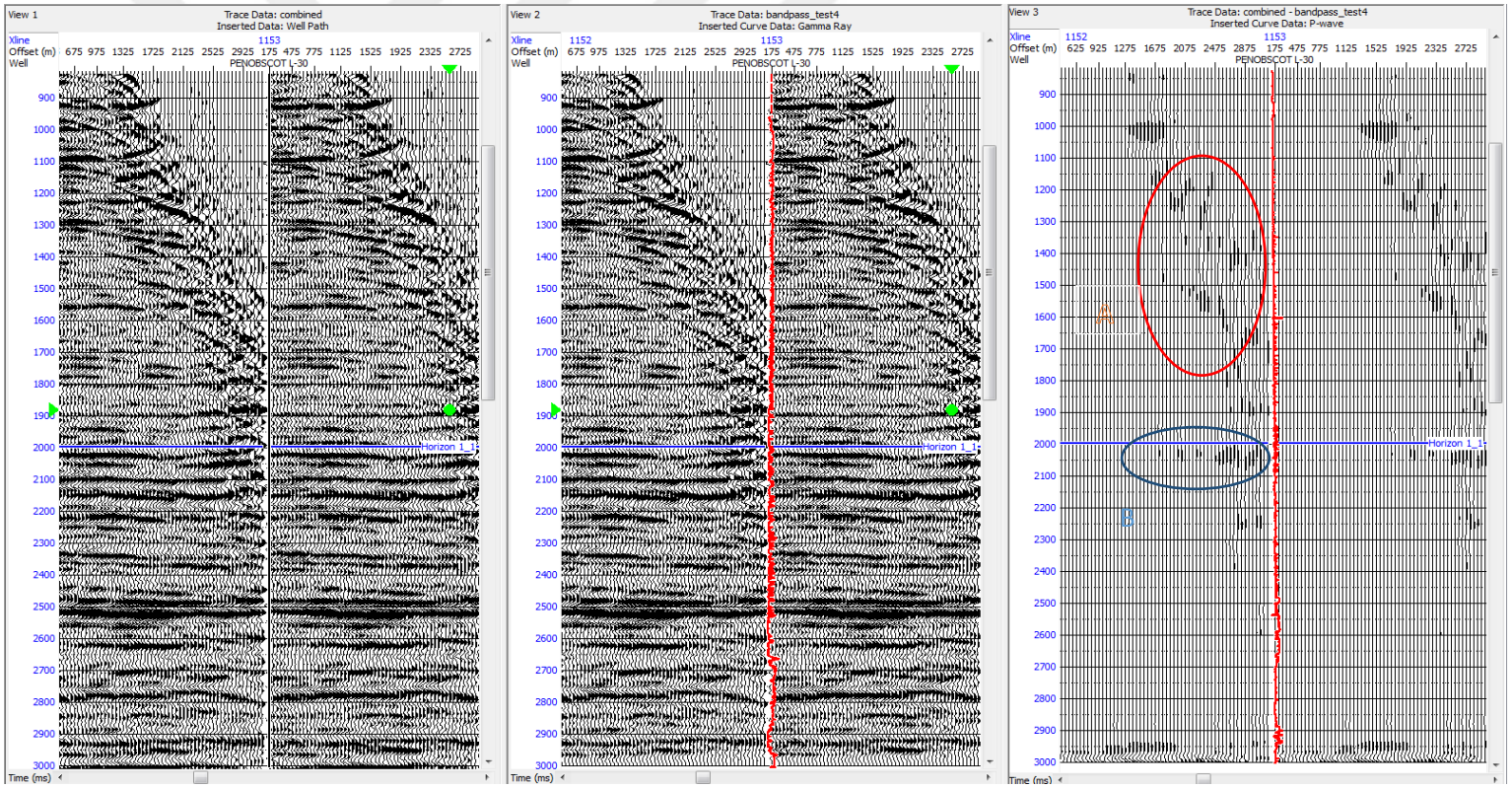


Figure 24: Bandpass filter test 4. Original prestack data, bandpass filtered data, and the rejected part of the data are shown respectively for Inline 1177 and crossline 1153. A shows rejected multiples and noise, while B shows the rejected real reflections.

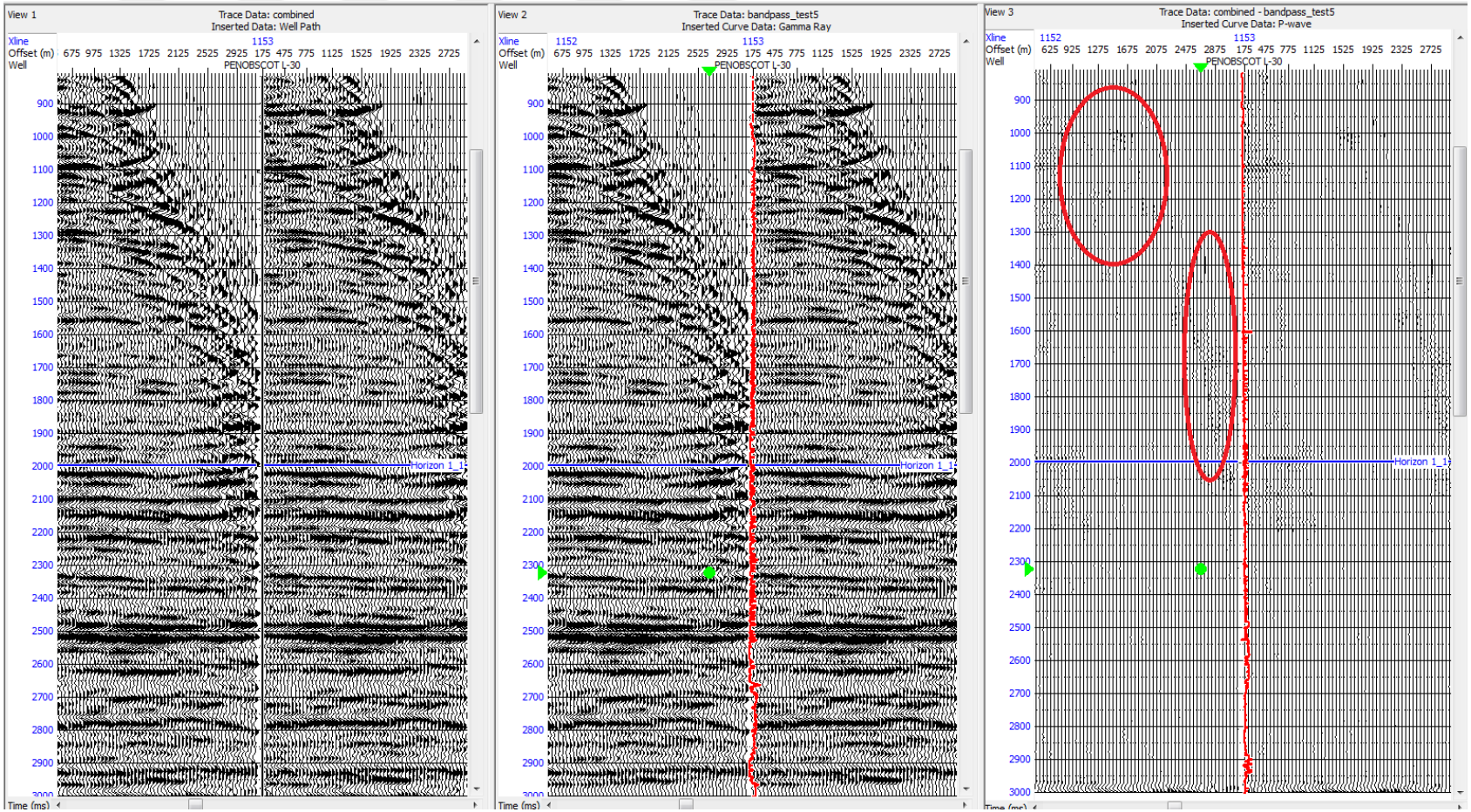


Figure 25: Bandpass filter test 5. Original prestack data, bandpass filtered data, and the rejected part of the data are shown respectively for Inline 1177 and crossline 1153. Here, the red circles show rejected noise from the data.

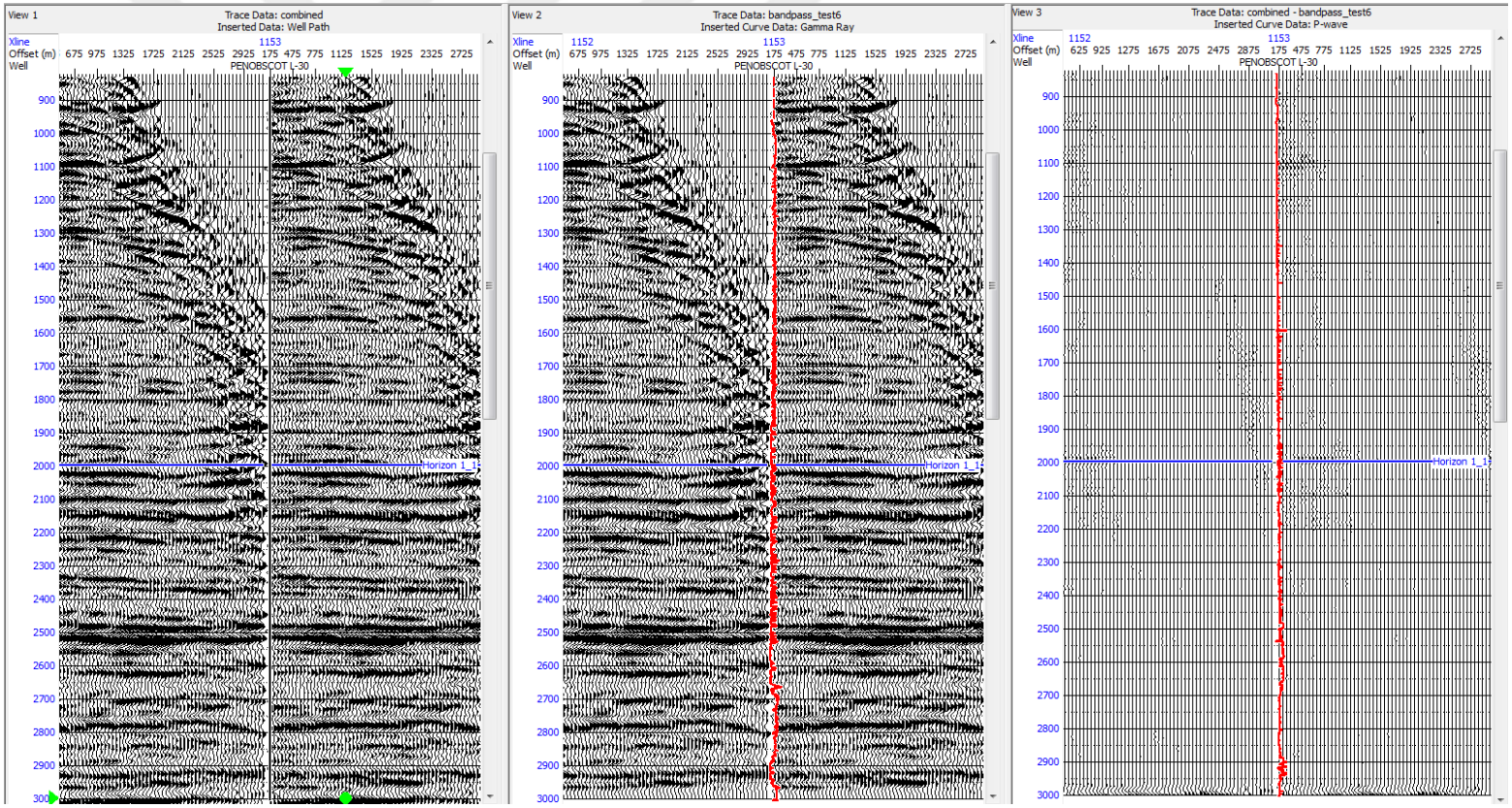


Figure 26: Bandpass filter test 6. Original prestack data, bandpass filtered data, and the rejected part of the data are shown respectively for Inline 1177 and crossline 1153. Here there is no significant rejected noise and real reflections.

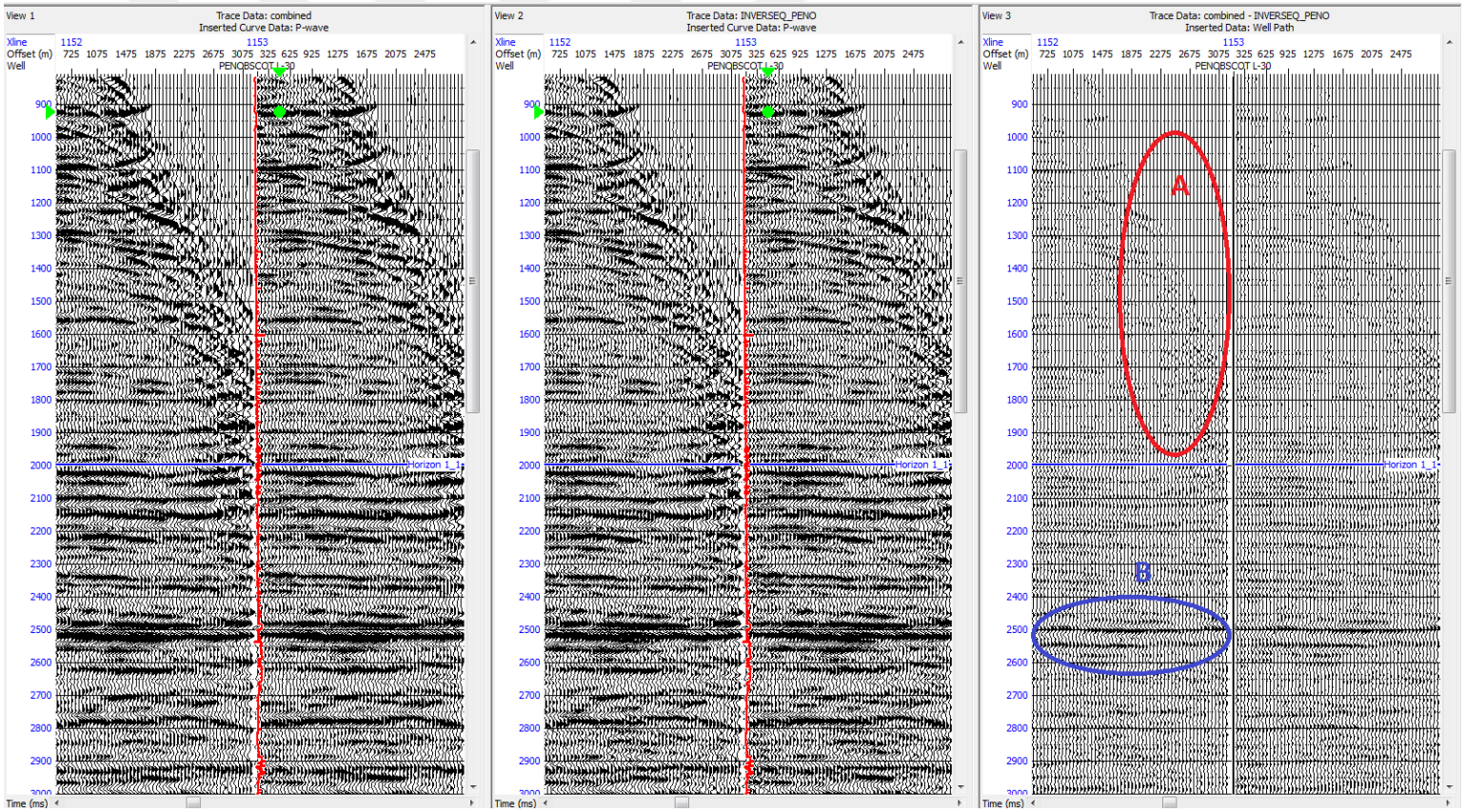


Figure 27: Inverse Q test 1. Original prestack data, inverse Q filtered data, and the rejected part of the data are shown respectively for Inline 1177 and crossline 1153. A shows multiples and noise added to the seismic, while B shows the added extra information in order to improve the data.

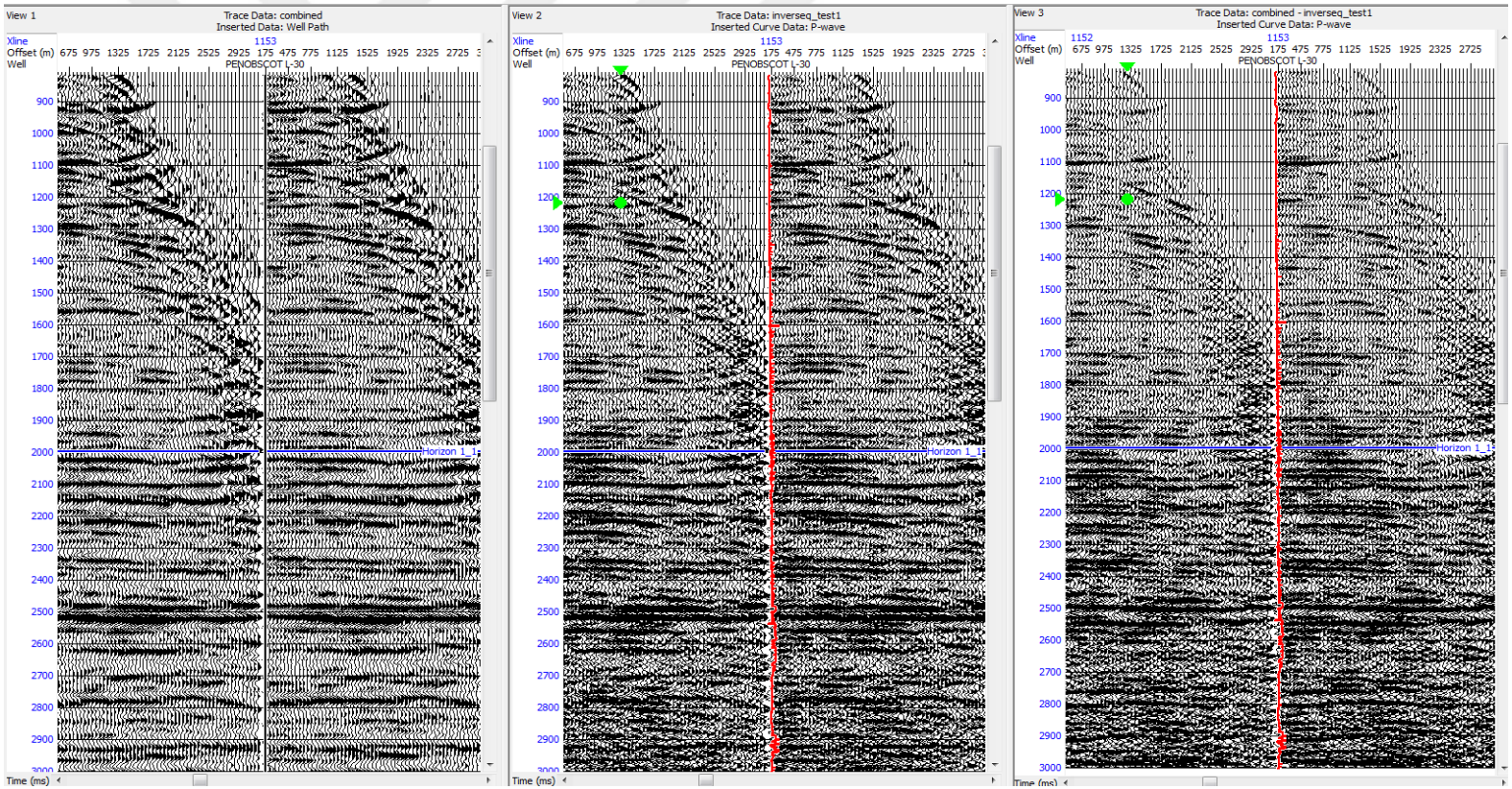


Figure 28: Inverse Q test 2. Original prestack data, inverse Q filtered data, and the rejected part of the data are shown respectively for Inline 1177 and crossline 1153.

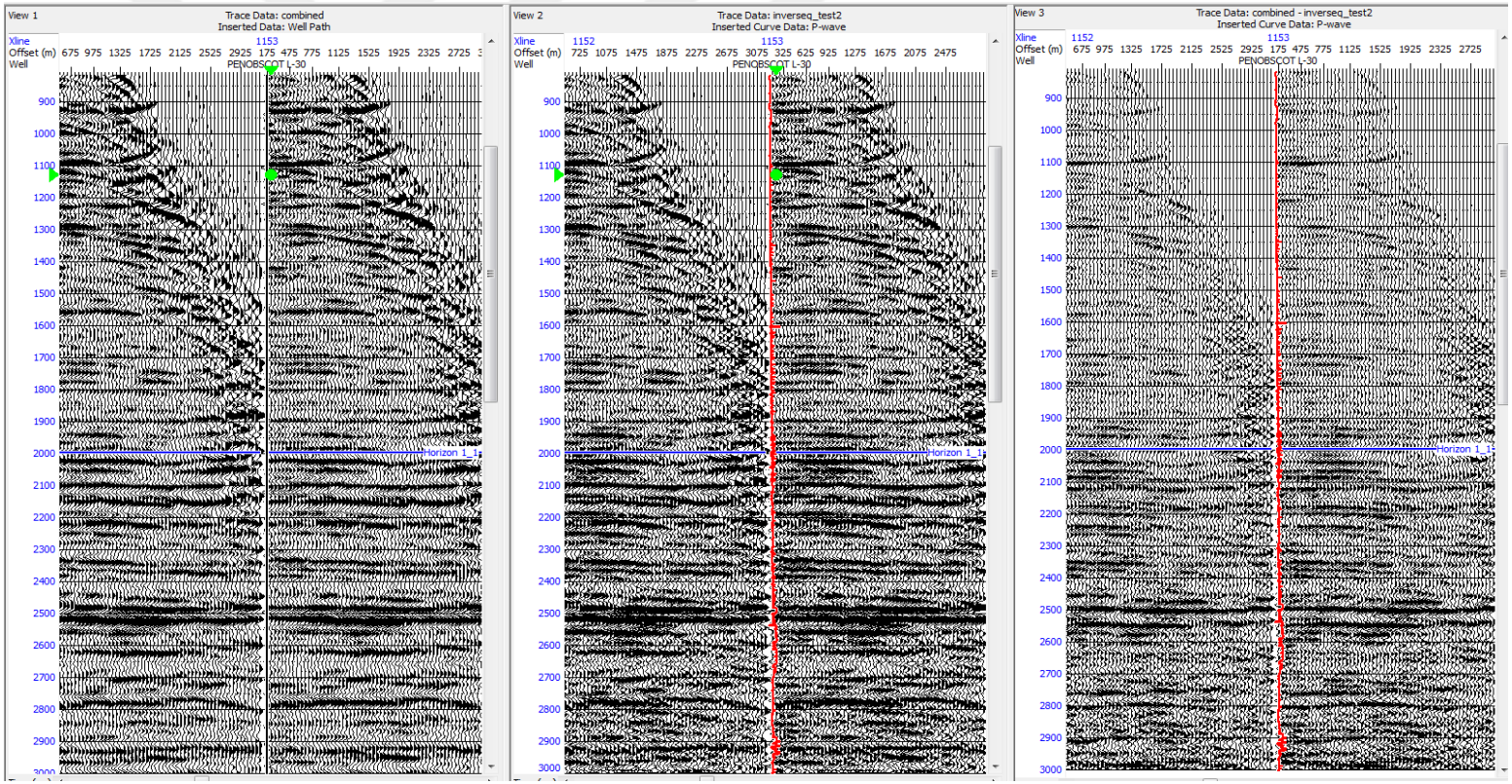


Figure 29: Inverse Q test 3. Original prestack data, inverse Q filtered data, and the rejected part of the data are shown respectively for Inline 1177 and crossline 1153.

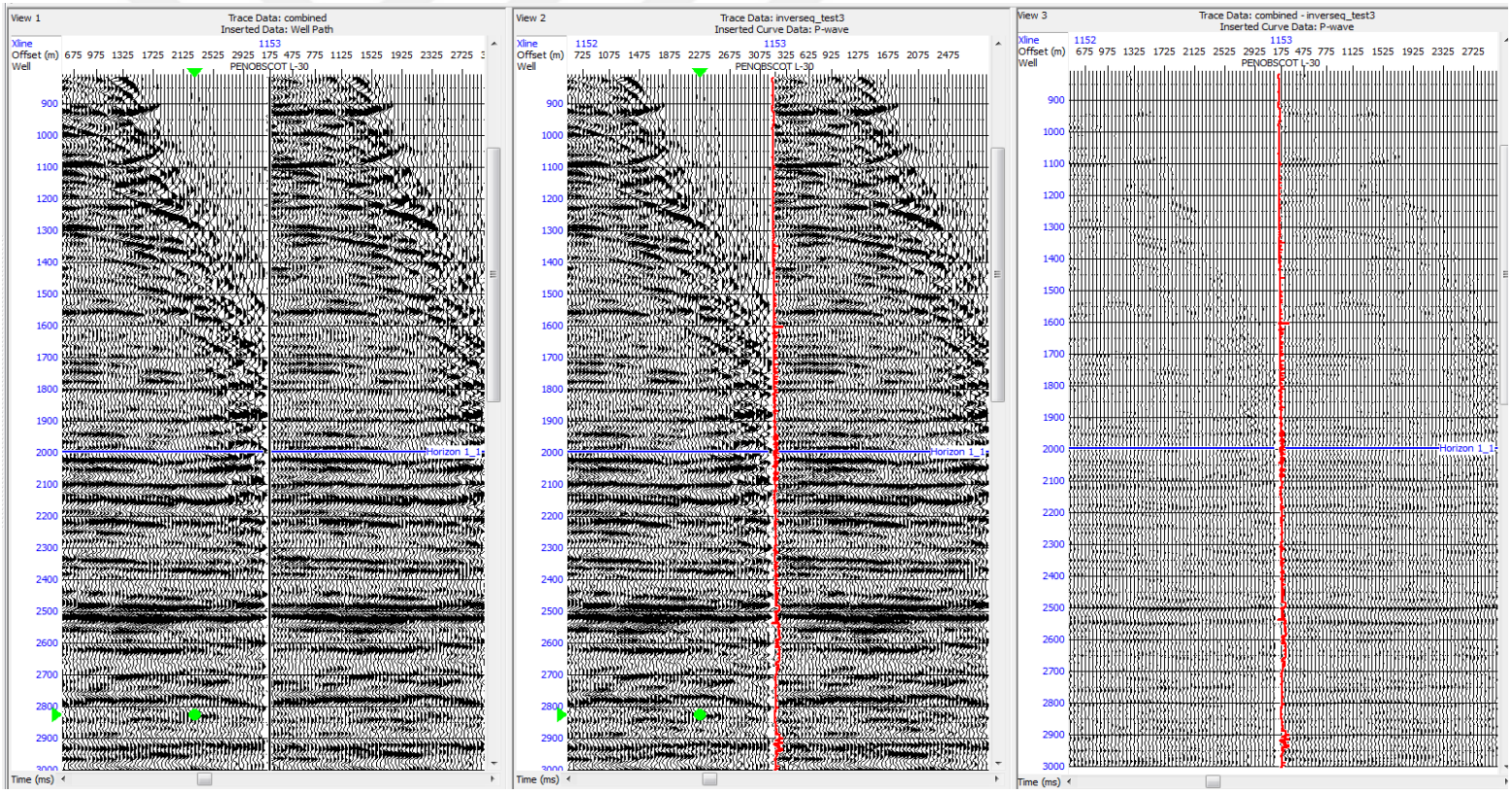


Figure 30: Inverse Q test 4. Original prestack data, inverse Q filtered data, and the rejected part of the data are shown respectively for Inline 1177 and crossline 1153.

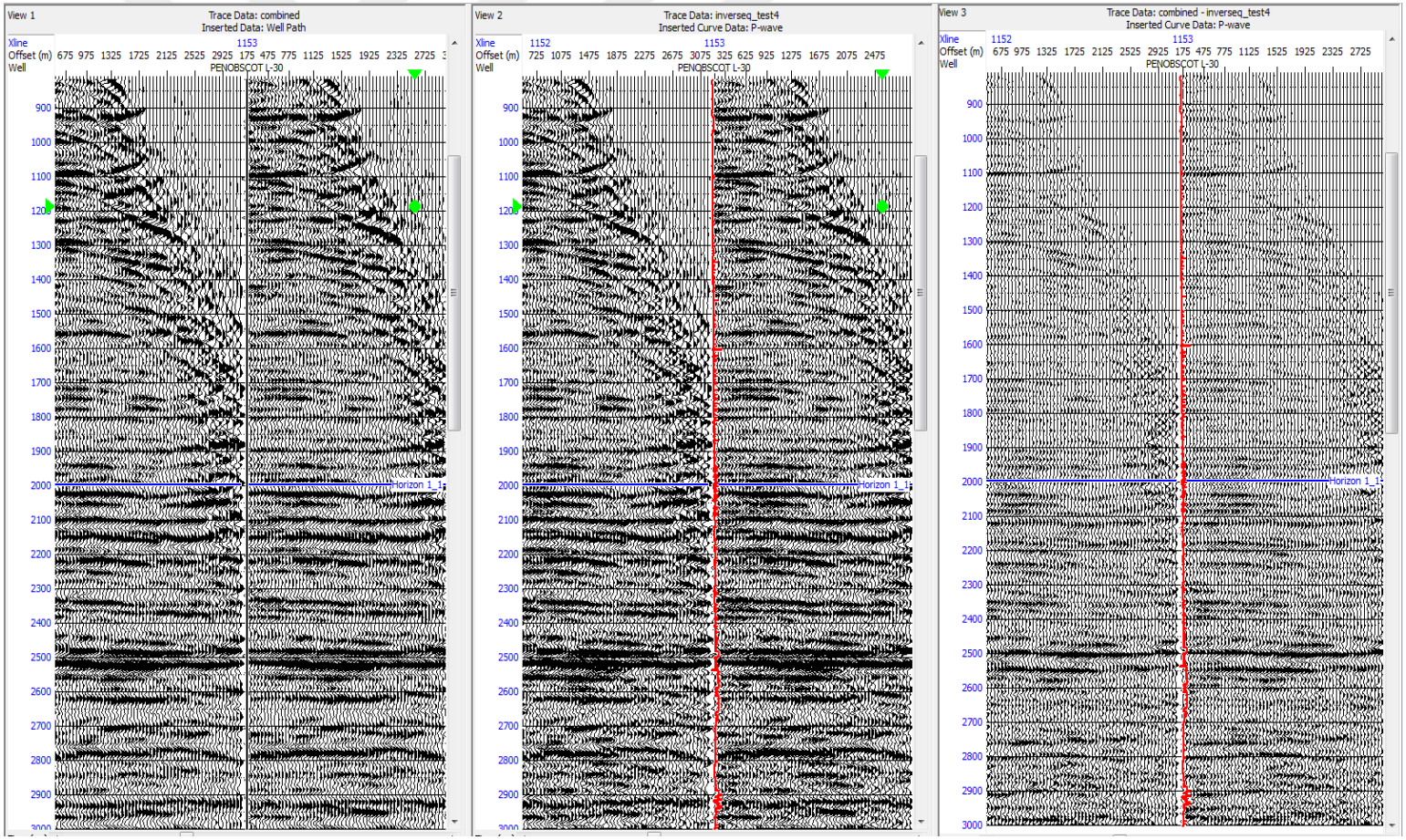


Figure 31: Inverse Q test 5. Original prestack data, inverse Q filtered data, and the rejected part of the data are shown respectively for Inline 1177 and crossline 1153.

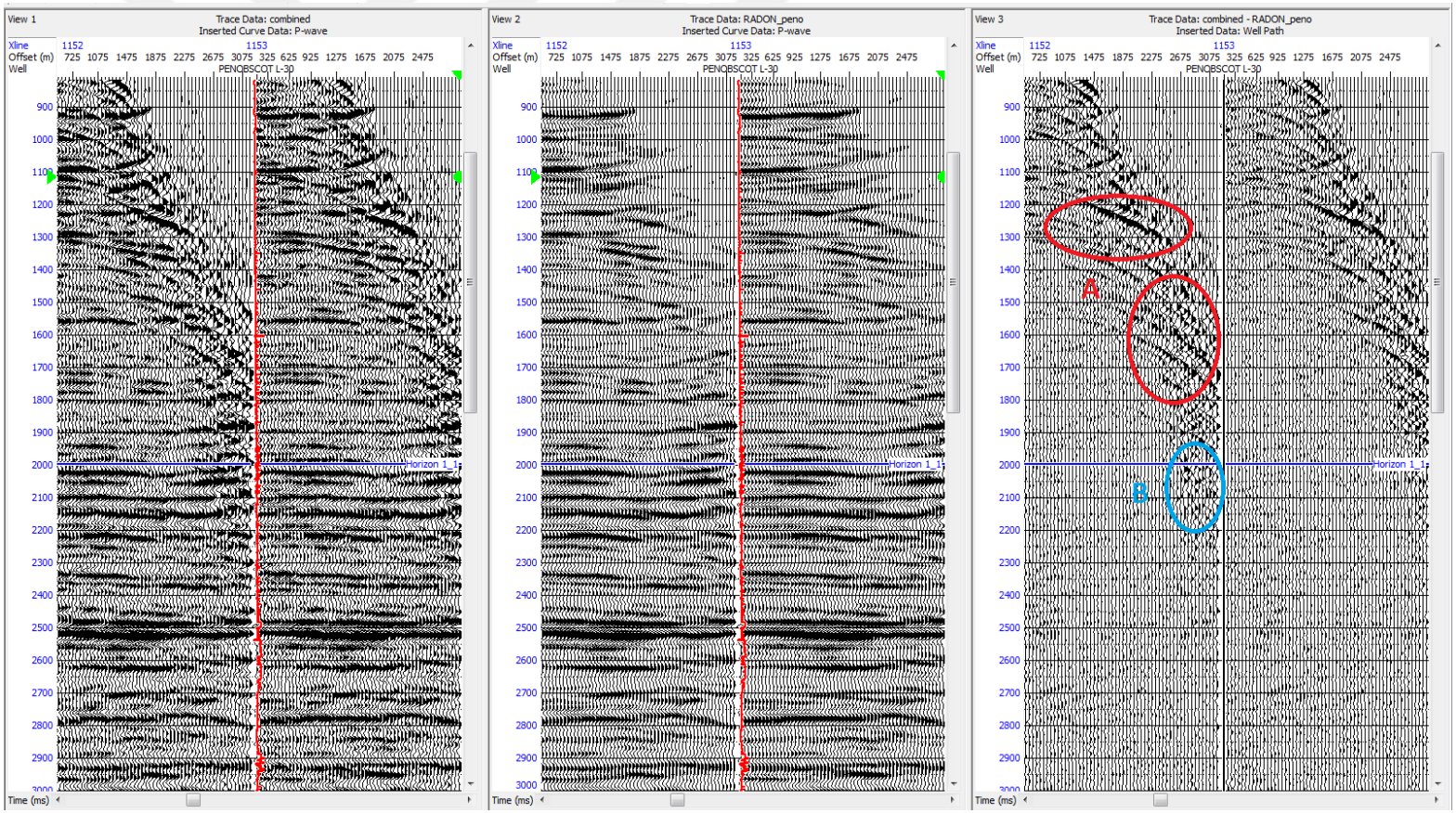


Figure 32: Radon Transform test 1. Original prestack data, radon transform filtered data, and the rejected part of the data are shown respectively for Inline 1177 and crossline 1153. Here A shows the multiples and noise rejected, while B shows the rejected primaries.

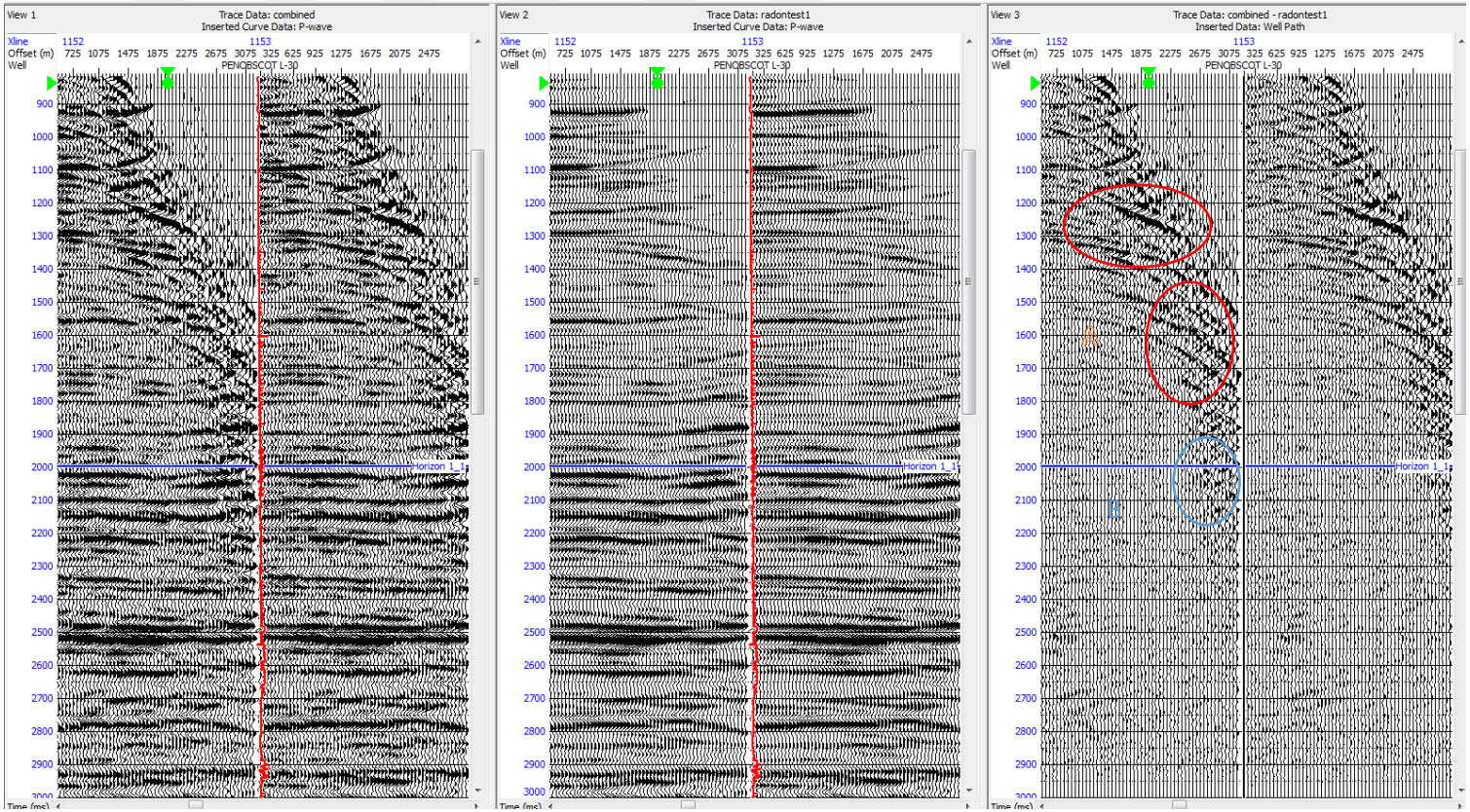


Figure 33: Radon Transform test 2. Original prestack data, inverse Q filtered data, and the rejected part of the data are shown respectively for Inline 1177 and crossline 1153. A shows the multiples and noise rejected, B shows the primaries.

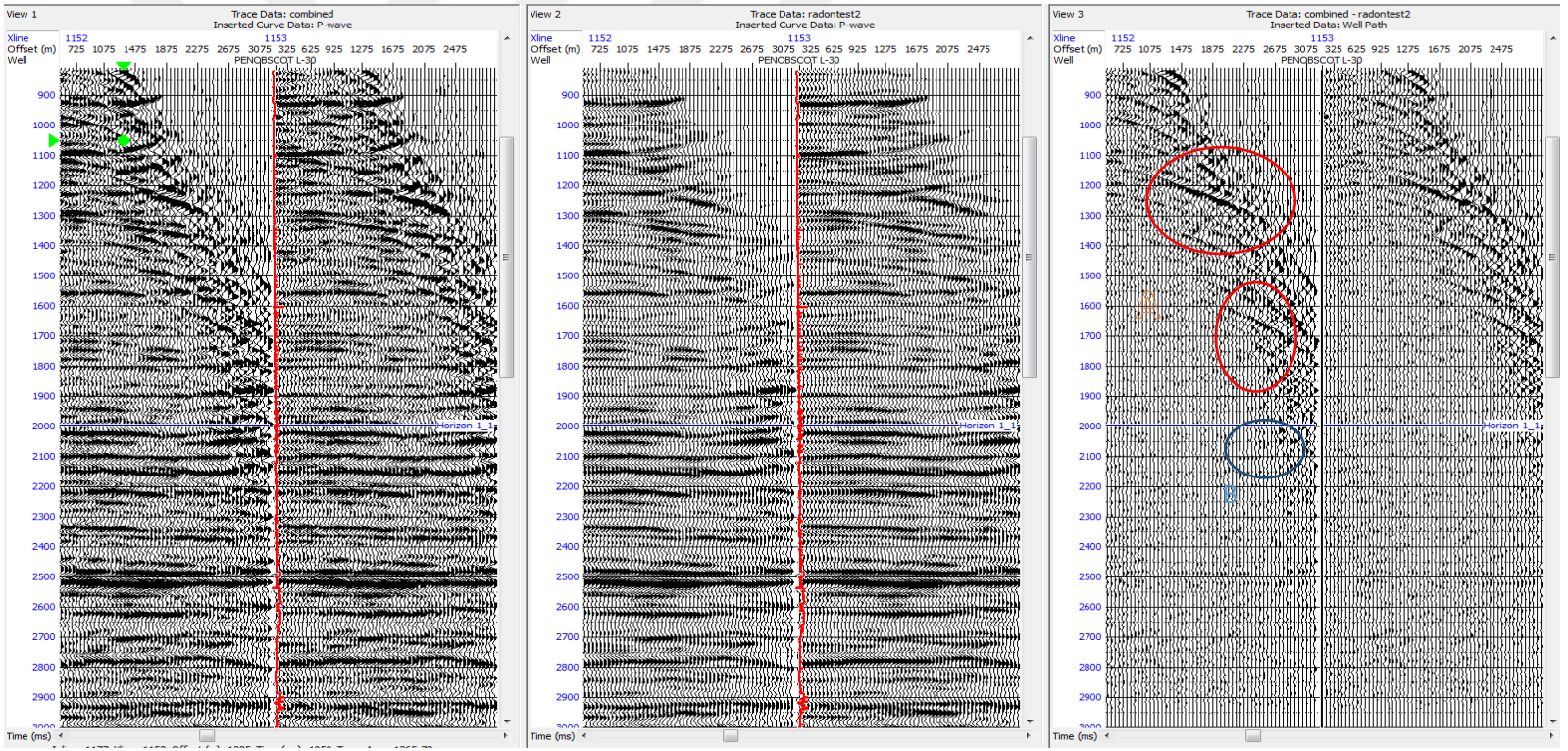


Figure 34: Radon Transform test 3. Original prestack data, inverse Q filtered data, and the rejected part of the data are shown respectively for Inline 1177 and crossline 1153. A shows the multiples and noise, while B shows rejected noise.

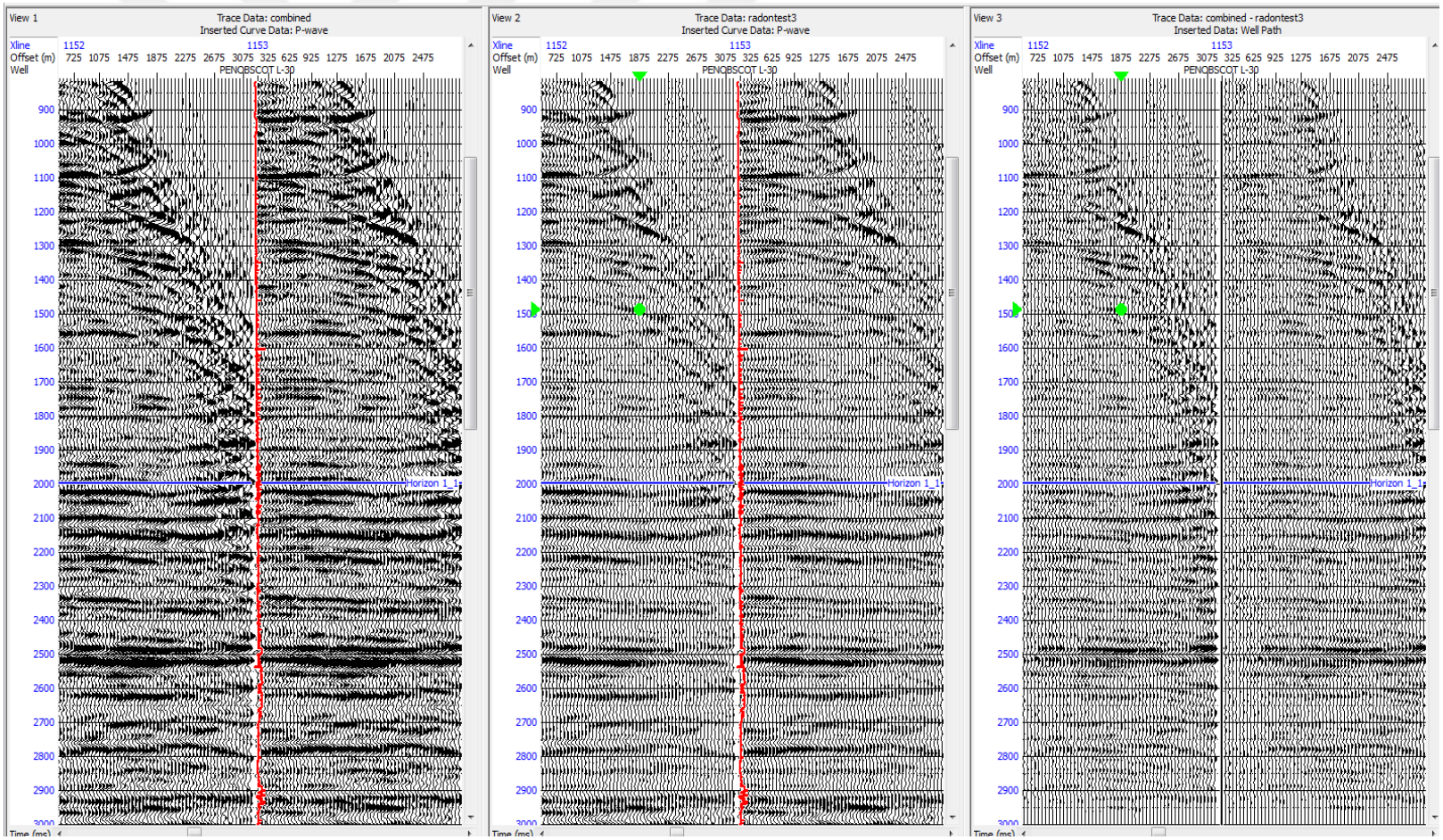


Figure 35: Radon Transform test 4. Original prestack data, inverse Q filtered data, and the rejected part of the data are shown respectively for Inline 1177 and crossline 1153.

**Copyright Permission**

**Figure 1 Google Image Copyright Permission**

Thanks for considering Google Maps, Google Earth and Street View for your project! These guidelines are for non-commercial use except for the limited use cases described below; if you want to use Google Maps, Google Earth, or Street View for other commercial purposes, please contact the Google Maps for Work sales team. "Commercial purposes" means "use for sale or revenue-generating purposes". We created this page to clarify questions we've received from users over the years regarding uses of our mapping tools in everything from marketing and promotional materials, films, television programs, books, academic journals, and much more. Generally speaking, as long as you're following our Terms of Service and you're attributing properly, we're cool with your using our maps and imagery; in fact, we love seeing all of the creative applications of Google Maps, Google Earth and Street View!

https://www.google.com/permissions/geoguidelines.html#generalguidelines